

Supporting Information

**Green-Light Induced Cycloadditions**

Philipp Kamm,<sup>abc</sup> James P. Blinco,<sup>\*ab</sup> Andreas-Neil Unterreiner,<sup>\*c</sup> and Christopher Barner-Kowollik<sup>\*ab</sup>

- a Centre for Materials Science, Queensland University of Technology (QUT), 2 George Street, Brisbane, QLD 4000, Australia.
- b School of Chemistry and Physics, Queensland University of Technology (QUT), 2 George Street, Brisbane, QLD 4000, Australia.
- c Molecular Physical Chemistry Group, Institute of Physical Chemistry, Karlsruhe Institute of Technology (KIT), Fritz-Haber-Weg 2, Geb. 30.44, 76131 Karlsruhe, Germany.

1. Supporting Figures .....	3
2. Methods and Instrumentation.....	11
2.1. Characterization Instruments .....	11
2.1.1. Nuclear Magnetic Resonance (NMR) spectroscopy.....	11
2.1.2. Liquid Chromatography Coupled Mass Spectrometry (LC-MS) .....	12
2.1.3. DMAC-Size Exclusion Chromatography (SEC) .....	12
2.1.4. Chromatography .....	13
2.1.5. UV/Vis and Fluorescence Spectroscopy.....	13
2.2. Photochemical Procedures .....	15
2.2.1. Laser Experiments.....	15
2.2.2. LED Experiments .....	22
2.3. Synthesis .....	24
2.3.1. Materials .....	24
2.3.2. Dimethylaminopyrene aryl tetrazole (APAT) .....	25
2.3.3. Maleimide end-capped poly(methyl)methacrylate .....	37
3. Supporting References.....	43

# 1. Supporting Figures

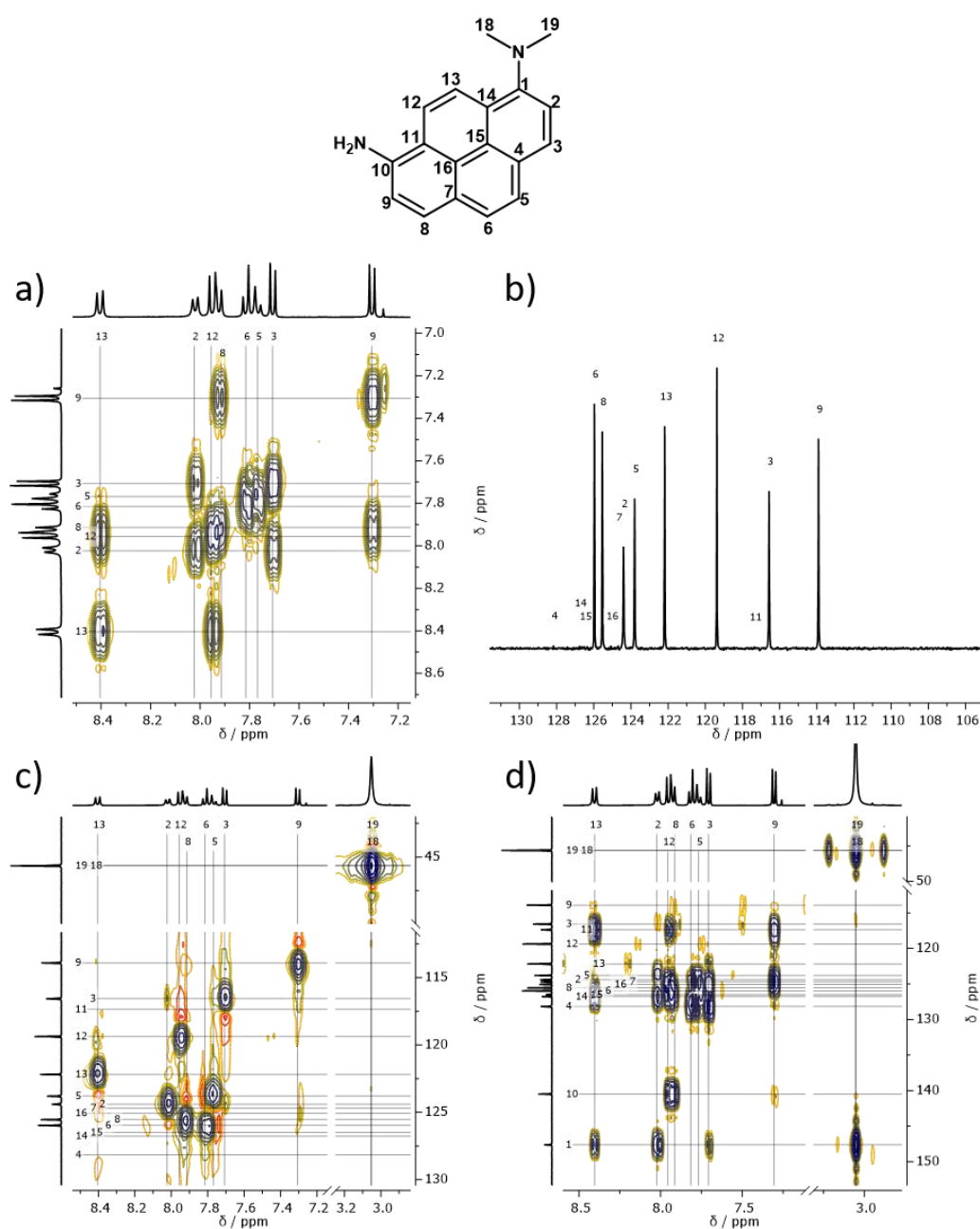


**Figure S 1** Determination of isomeric structure of the precursor **2** for the synthesis of APAT (refer to **2.3.2**). a) Correlation spectroscopy (COSY), b) DEPTQ 135 experiment, c) heteronuclear single quantum correlation (HSQC) experiment, d) heteronuclear multiple bond correlation (HMBC) experiment. For clarity, only the relevant correlations in the aromatic region, as well as the  $-\text{NMe}_2$  signals, are shown and the rest of the spectra is omitted. For  $^1\text{H}$ - and  $^{13}\text{C}$ -NMR spectra refer to **2.3.2**.

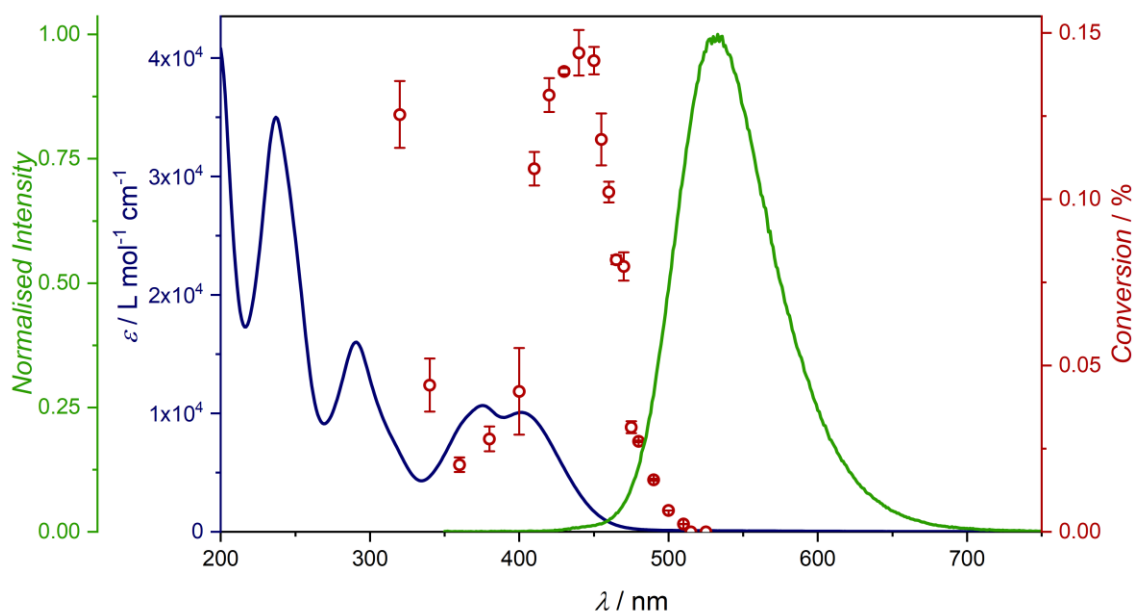


**Figure S 2** **Left axis a:** Normalised fluorescence spectrum of APAT in MeCN after excitation at 335 nm. **Left axis b:** Full absorption spectrum of APAT in MeCN. **Right axis:** Action plot of the NITEC reaction between APAT and diethylfumarate.

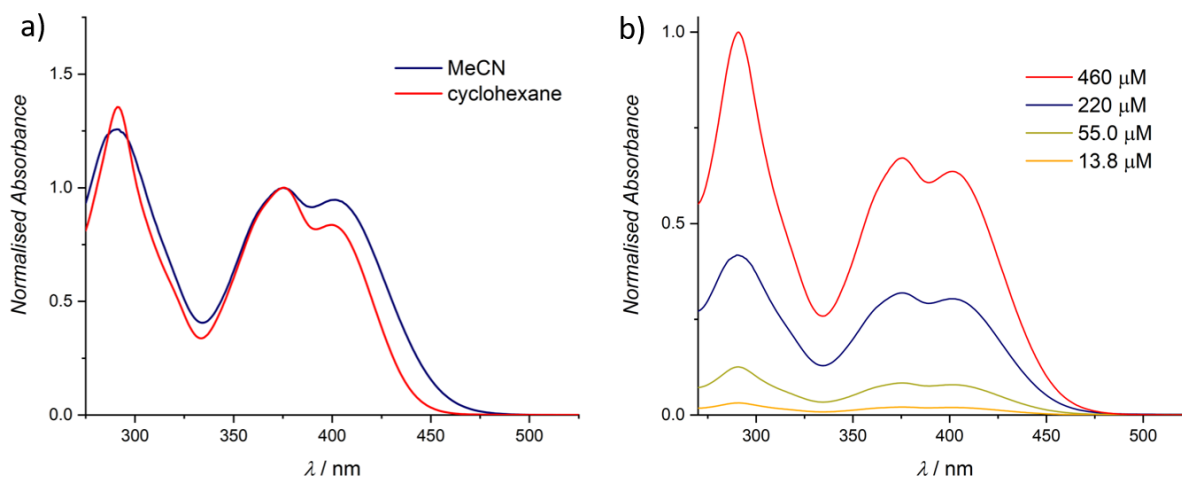


**Figure S 3** a) Normalised absorption spectra of APAT in cyclohexane and acetonitrile. Red-shift and relative intensity of the higher-wavelength absorption band increases with solvent polarity. b) Concentration-dependent absorption measurements. The 460  $\mu\text{M}$  sample was measured in a 2 mm cuvette due to low transmittance; All other spectra were measured in 10 mm cuvettes.

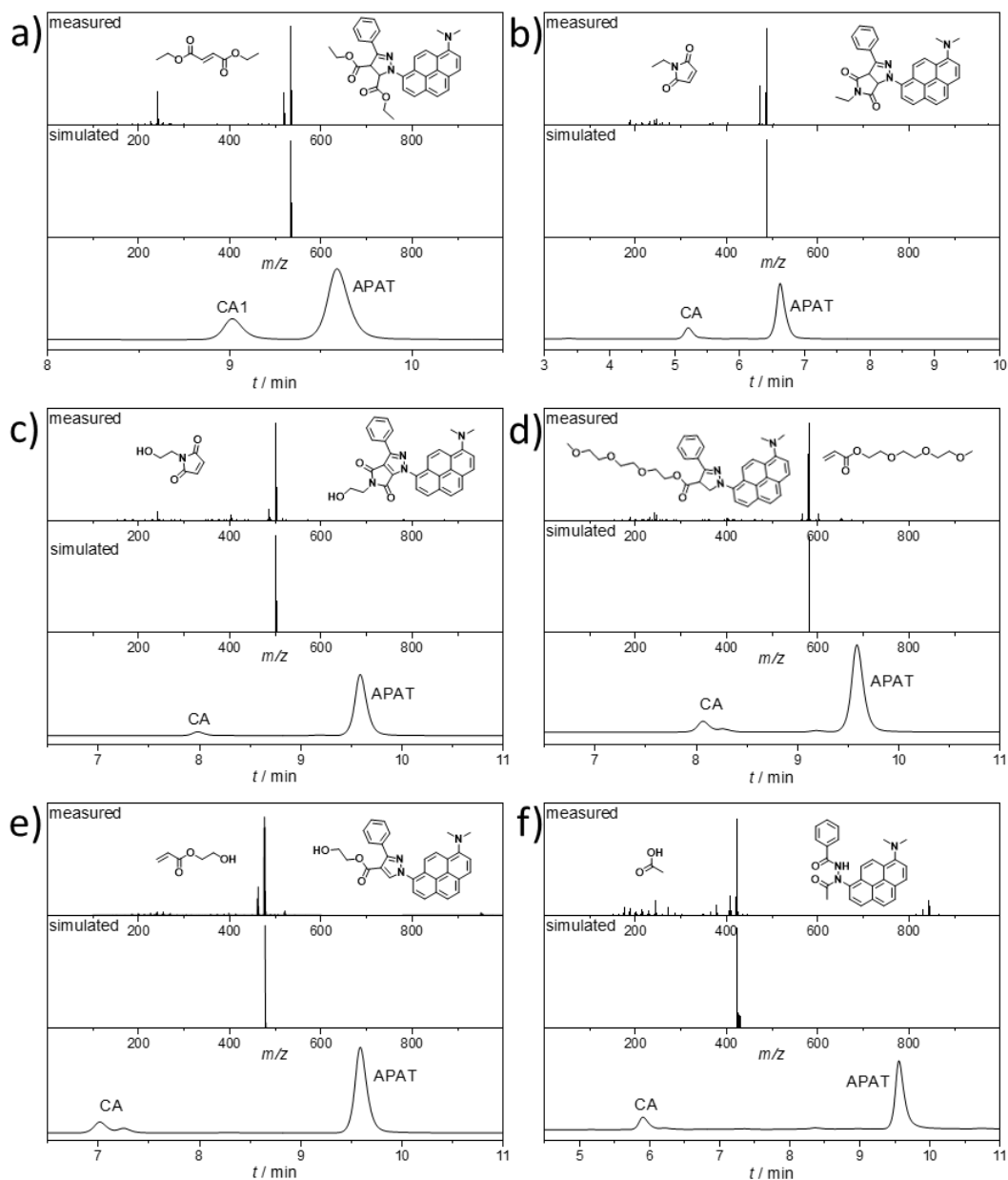


**Figure S 4** LC-MS analysis of NITEC and NICAL (nitrile imine-carboxylic acid ligation) reactions of APAT with various electron deficient double bonds, as well as acetic acid. The schemes show the dipolarophile and the respective cycloadducts. The chromatograms of c) and d) show two species of CA, since cycloadducts can be formed as head-to-head or head-to-tail regio-isomers, of which only one is depicted in the scheme. a) Diethylfumarate:  $[M-H]^+ = 534.2374$ , found: 534.2387 ( $\Delta m/z = -2.4$  ppm). b) *N*-ethylmaleimide:  $[M-H]^+ = 487.2129$ , found: 487.2120 ( $\Delta m/z = -1.8$  ppm). c) *N*-(2-hydroxyethyl) maleimide:  $[M-H]^+ = 501.1921$ , found: 501.1920 ( $\Delta m/z = -0.2$  ppm). d) 2-(2-(2-methoxyethoxy)ethoxy)ethyl acrylate:  $[M-H]^+ = 580.2806$ , found: 580.2792 ( $\Delta m/z = -2.4$  ppm). e) 2-hydroxyethyl acrylate:  $[M-H]^+ = 476.1969$ , found: 476.1969 ( $\Delta m/z = 0$  ppm). f) Acetic acid:  $[M-H]^+ = 422.1863$ , found: 422.1899 ( $\Delta m/z = 8.5$  ppm).

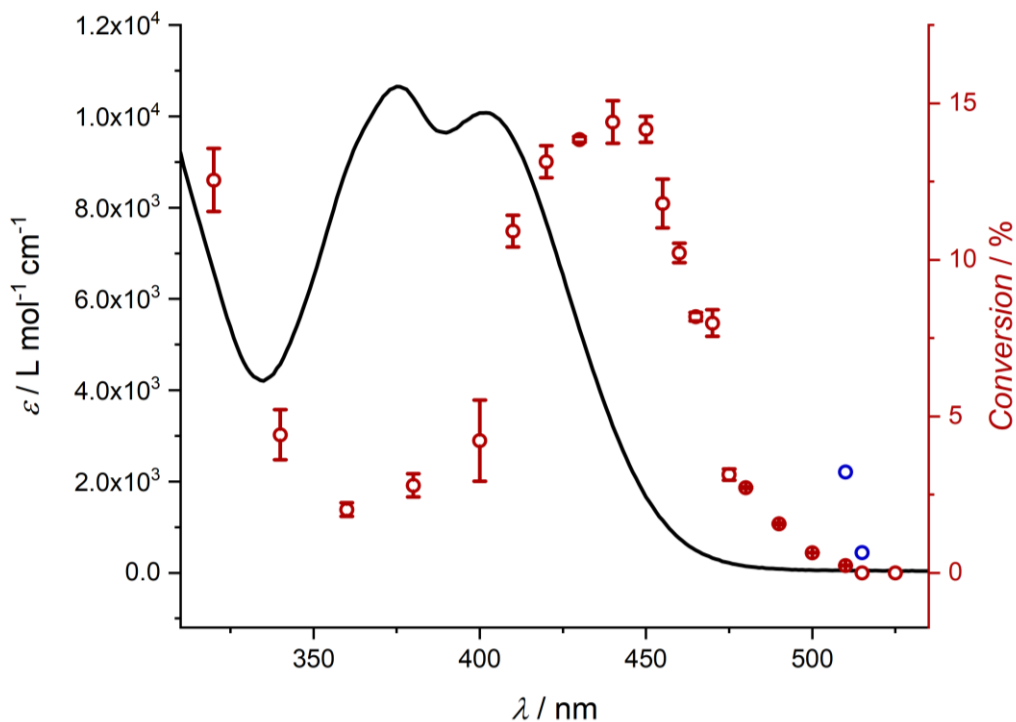


**Figure S 5** Overlay of the absorption profile of APAT (**left y-axis**) and the extended wavelength-dependent reactivity profile of the photo-induced NITEC reaction between APAT and diethylfumarate (**right y-axis**). Two data points (**blue**) added after 25-fold increase of incident photon number, corresponding to 3.0 % (510 nm) and 0.6 % (515 nm) conversion.

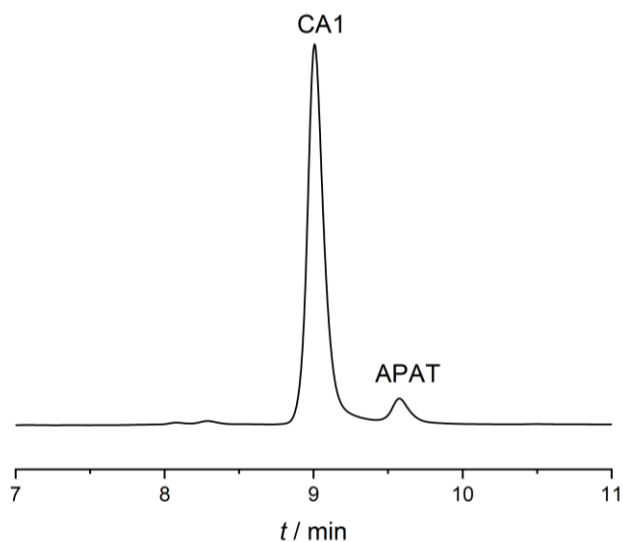


**Figure S 6** LC-MS chromatogram after NITEC reaction between APAT and diethylfumarate driven to high conversion (89 %) after laser irradiation with 465 nm light.

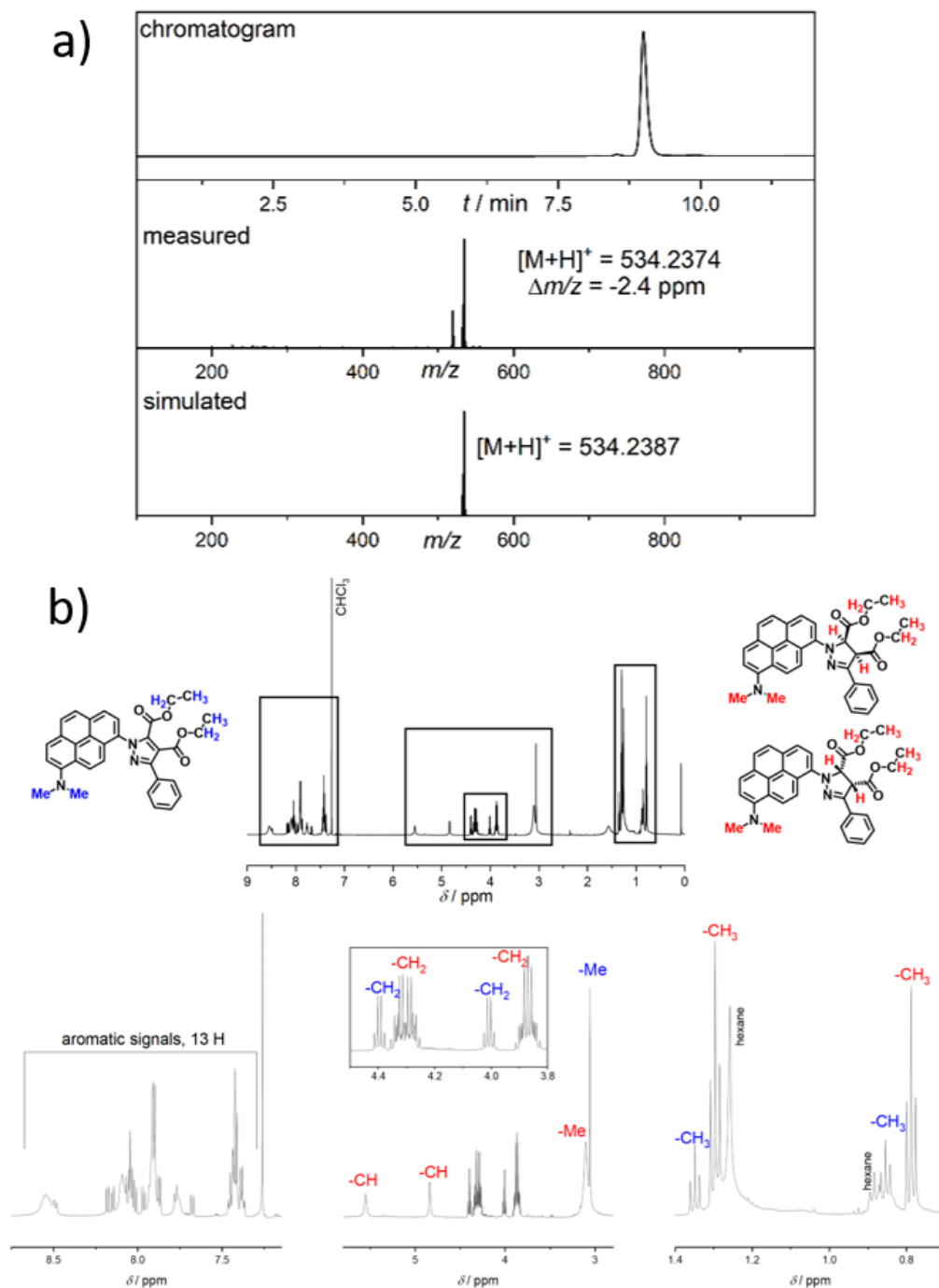


**Figure S 7** Analysis of CA1. a) LC-MS chromatogram and mass spectrum confirm purity of isolated CA1. A second peak in the mass spectrum ( $m/z$  difference 15.0220) is due to cleaving of a  $\text{CH}_3$  group in the ionization process of the ESI-MS. b)  $^1\text{H}$ -NMR spectrum with peak assignments. Due to overlapping peaks, no peaks were assigned in the aromatic region.

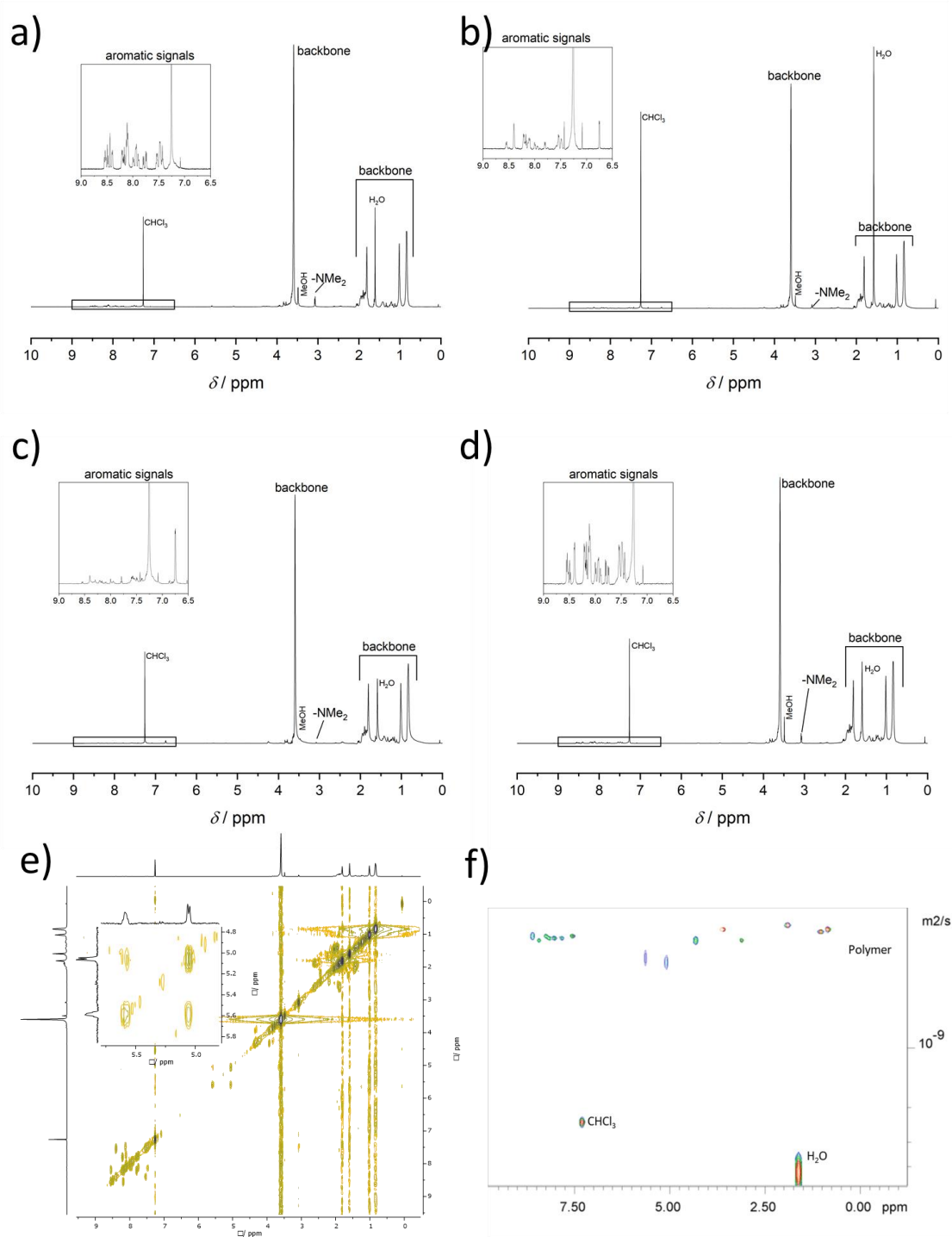


**Figure 8**  $^1\text{H-NMR}$  spectra of CA2 after NITEC reaction between APAT and maleimide end-capped PMMA, and purification through preparative SEC and precipitation. a) 10 W LED at 452 nm for 2.5 h (100 % conversion) b) 10 W LED at 500 nm for 3.7 h (50 % conversion). c) 10 W LED at 515 nm for 4.3 h (conversion could not be quantified, ca. 1-5 %). d) 10 W LED at 500 nm for 48 h (100 % conversion) e) COSY of CA2 after 500 nm irradiation for 48 h. Inlet: Zoom onto dihydropyrazole peaks of the non-rearomatized cycloadduct. f) DOSY of CA2 after 500 nm irradiation for 48 h. Results confirm that the aromatic end-group as well as the dihydropyrazole peaks are attached to the polymer chain.

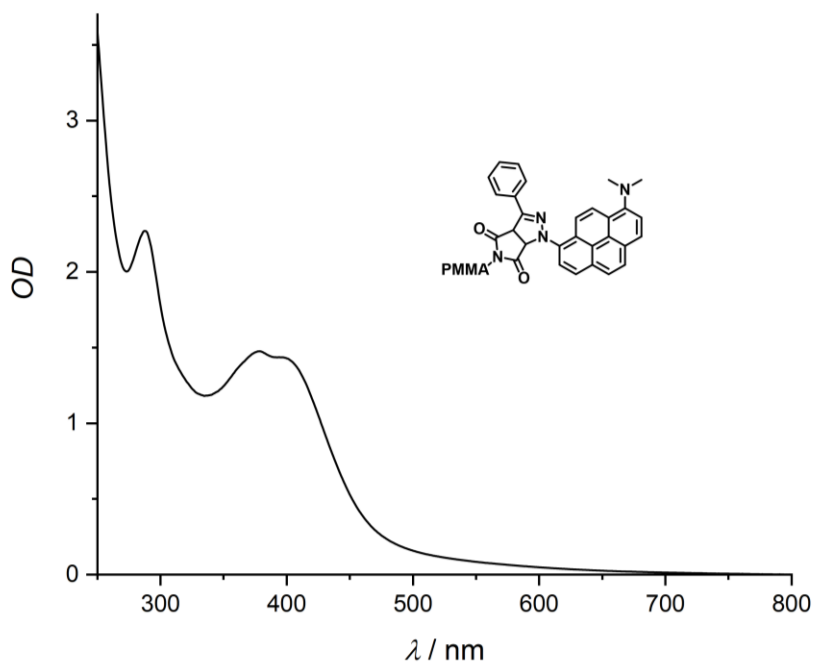


**Figure S 9** Absorption spectrum of CA2 in MeCN.

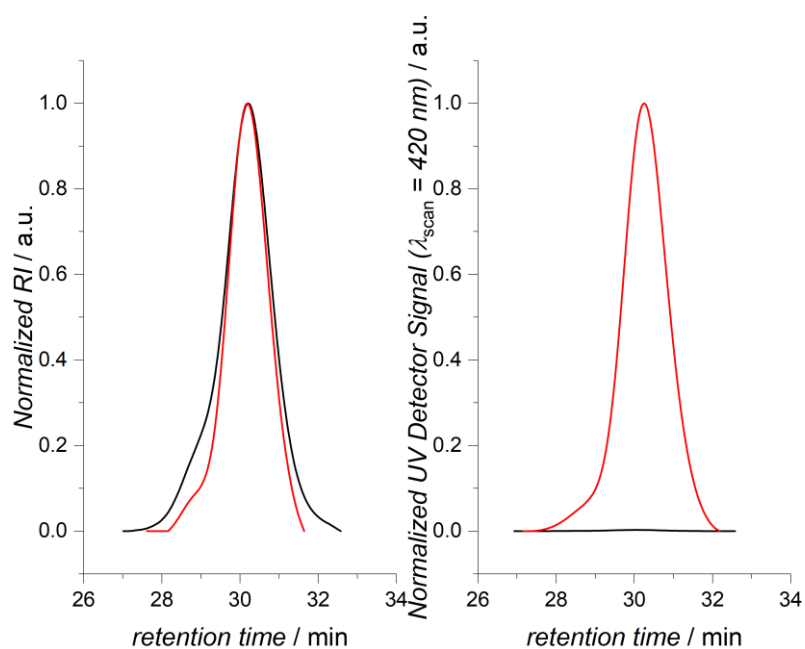


**Figure S 10** SEC traces **before** and **after** irradiation at 500 nm for 48 h (100 % conversion). Left graph: RI trace displays a slight shift to lower retention times, corresponding to higher molecular weight (**before**:  $M_n = 4.7$  kDa,  $\mathcal{D} = 1.16$ , **after**:  $M_n = 4.8$  kDa,  $\mathcal{D} = 1.09$ ). Right graph: UV-Vis scan at 420 nm shows no signal before the reaction. After ligation and formation of CA2 the shape of the UV-Vis trace follows the RI trace.

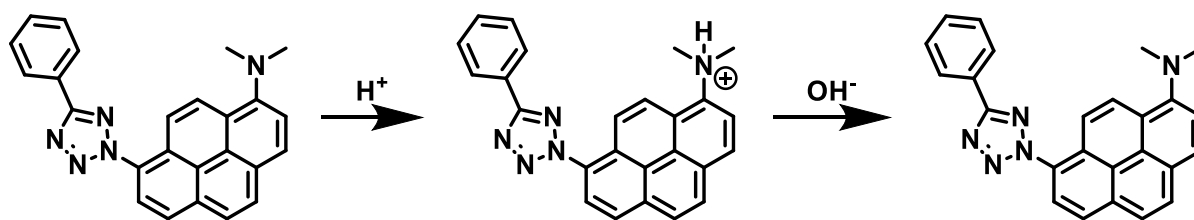
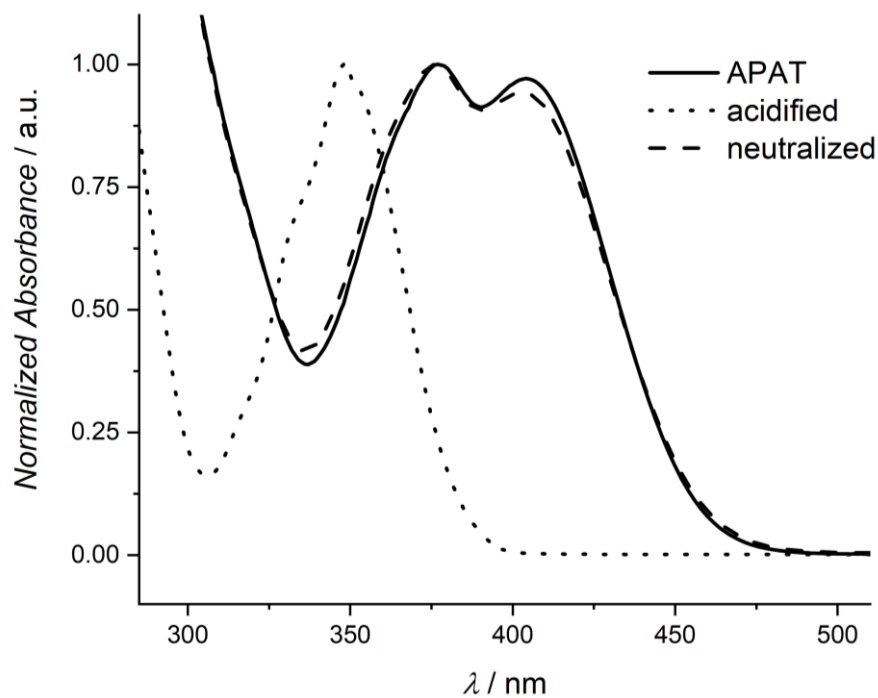


**Figure S 11** pH-responsivity of the absorption spectrum of APAT. Spectra measured in MeCN. After acidification with HCl absorption shows hypsochromic shift by ca. 50 nm. Absorption can be recovered by neutralizing the solution with triethylamine. Slight change in the recovered absorption spectrum may be due to change of solvent polarity after addition of HCl and TEA. We observed a strong solvent effect of the absorption spectrum for different solvents.

## 2. Methods and Instrumentation

### 2.1. Characterization Instruments

#### 2.1.1. Nuclear Magnetic Resonance (NMR) spectroscopy

$^1\text{H}$ -NMR,  $^{13}\text{C}$ -NMR as well as DEPT 135, COSY, HSQC and HMBC-spectra were recorded on a Bruker System 600 Ascend LH, equipped with a BBO-Probe (5 mm) with z-gradient ( $^1\text{H}$ : 600.13 MHz,  $^{13}\text{C}$  150.90 MHz). Resonances are reported in parts per million (ppm) relative to tetramethylsilane (TMS). The  $\delta$ -scale was calibrated to the respective solvent signal of  $\text{CHCl}_3$  or DMSO for  $^1\text{H}$  spectra and for  $^{13}\text{C}$  spectra on the middle signal of the  $\text{CDCl}_3$  triplet or the DMSO quintet. The annotation of the signals is based on HSQC-, COSY- and DEPT-experiments.

#### **Diffusion Ordered Spectroscopy (DOSY)**

DOSY experiments based on  $^1\text{H}$  NMR were performed in  $\text{CDCl}_3$  at 296 K on a Bruker 400 UltraShield spectrometer equipped with a Quattro Nucleus Probe (QNP) with an operating frequency of 400 MHz ( $^1\text{H}$ ). A sequence with longitudinal eddy current delay (LED) using bipolar gradients was employed in order to compensate eddy currents. Bipolar gradient  $\delta$  and a diffusion delay  $\Delta$  were determined separately for each sample. Gradient strength was linearly incremented from 2 % at 0.96 G to 95 % at 45.7 G in 24 steps. The obtained data was processed with TopSpin 4.0.6 and Dynamics Center 2.5.3.

After Fourier transform of the 1D spectra, the signal decay along the gradients  $G$  was fitted to

$$(G) = I_0 * e^{-D * G^2 * \gamma^2 * \delta^2 * (\Delta - \frac{\delta}{3})} * 10^4$$

with the gyromagnetic ratio  $\gamma$  and the full signal intensity  $I_0$ .

## 2.1.2. Liquid Chromatography Coupled Mass Spectrometry (LC-MS)

Liquid-chromatography coupled mass spectrometry (LC-MS) measurements were performed on an UltiMate 3000 UHPLC System (Dionex, Sunnyvale, CA, USA) consisting of a pump (LPG 3400SZ), autosampler (WPS 3000TSL) and a temperature-controlled column compartment (TCC 3000). Separation was performed on a C18 HPLC column (Phenomenex Luna 5 $\mu$ m, 100 Å, 250  $\times$  2.0 mm) operating at 40 °C. Gradient-free acetonitrile was used as eluent at a flow rate of 0.40 mL $\cdot$ min<sup>-1</sup>. The flow was split in a 9:1 ratio, where 90 % of the eluent was directed through a DAD UV-detector (VWD 3400, Dionex) and 10 % was infused into the electrospray source. Spectra were recorded on an LTQ Orbitrap Elite mass spectrometer (Thermo Fisher Scientific, San Jose, CA, USA) equipped with a HESI II probe. The instrument was calibrated in the  $m/z$  range 74-1822 using premixed calibration solutions (Thermo Scientific). A constant spray voltage of 3.5 kV, a dimensionless sheath gas and a dimensionless auxiliary gas flow rate of 5 and 2 were applied, respectively. The capillary temperature and was set to 300 °C, the S-lens RF level was set to 68, and the aux gas heater temperature was set to 100 °C. Samples were prepared at concentration of 0.5 mg mL<sup>-1</sup> in MeCN and filtered through 0.22  $\mu$ m PTFE membrane filters prior to injection.

## 2.1.3. DMAC-Size Exclusion Chromatography (SEC)

The SEC measurements were conducted on a PSS SECurity<sup>2</sup> system consisting of a PSS SECurity Degasser, PSS SECurity TCC6000 Column Oven (60 °C), PSS GRAM Column Set (8x150 mm 10  $\mu$ m Precolumn, 8x300 mm 10  $\mu$ m Analytical Columns, 1000 Å, 1000 Å and 30 Å) and an Agilent 1260 Infinity Isocratic Pump, Agilent 1260 Infinity Standard Autosampler, Agilent 1260 Infinity Diode Array and Multiple Wavelength Detector (A: 254 nm, B: 360 nm), Agilent 1260 Infinity Refractive Index Detector (35 °C). HPLC grade DMAc, 0.01 M LiBr, is used as eluent at a flow rate of 1 mL $\cdot$ min<sup>-1</sup>. Narrow disperse linear poly(styrene) ( $M_n$ : 266 g $\cdot$ mol<sup>-1</sup> to 2.52 $\times$ 10<sup>6</sup> g $\cdot$ mol<sup>-1</sup>) and poly(methyl methacrylate) ( $M_n$ :

202 g·mol<sup>-1</sup> to 2.2x10<sup>6</sup> g·mol<sup>-1</sup>) standards (*PSS ReadyCal*) were used as calibrants. All samples were passed over 0.22 µm PTFE membrane filters. Molecular weight and dispersity analysis was performed in *PSS WinGPC UniChrom* software (version 8.2).

#### 2.1.4. Chromatography

Flash chromatography was performed on a *Interchim XS420+* flash chromatography system consisting of a SP-in-line filter 20-µm, an UV-VIS detector (200-800 nm) and a *SoftA Model 400 ELSD* (55 °C drift tube temperature, 25 °C spray chamber temperature, filter 5, EDR gain mode) connected via a flow splitter (*Interchim Split ELSD F04590*). The separations were performed using a *Interchim* dry load column (liquid injection) and a *Interchim Puriflash Silica HP 30 µm* column or *Interchim Puriflash Silica HP 15 µm* column (were indicated).

#### 2.1.5. UV/Vis and Fluorescence Spectroscopy

##### **UV-Vis Spectroscopy**

UV-Vis spectra were recorded on a Shimadzu UV-2700 spectrophotometer equipped with a CPS-100 electronic temperature control cell positioner. Samples were prepared in solvent MeCN and measured in 10 mm Hellma Analytics quartz high precision cells at 25 °C. Molar absorption coefficients were obtained by measuring spectra at various concentrations and applying Beer-Lambert's law to calculate a linear fit:

$$OD = \varepsilon * d * c$$

##### **Fluorescence Spectroscopy**

Fluorescence spectra were measured using a Cary Eclipse Fluorescence Spectrophotometer from Agilent Technologies. Voltage was set to medium and the excitation wavelength was set to 430 nm with an excitation and emission slit of 5 nm (scan rate 600 nm min<sup>-1</sup>). Scan-range was 440-800 nm.

Samples were measured at ambient temperature in Hellma Analytics quartz high precision cells with a path length of 10 mm.

Fluorescence quantum yields were measured using Coumarin 307 in EtOH as a fluorescence standard ( $\Phi_f = 0.56$ ), with excitation wavelength 395 nm, using the following formula:

$$\Phi = \Phi_R * \frac{I}{I_R} * \frac{1 - 10^{-A_R}}{1 - 10^{-A}} * \frac{n^2}{n_R^2}$$

where  $\Phi$  is the fluorescence quantum yield of compound,  $I$  is the integral of the fluorescence spectrum,  $A$  is the absorbance of the sample and  $n$  is the refractive index of the solvent. Index R indicates the same entries for the reference sample (C307 in EtOH).

## 2.2. Photochemical Procedures

### 2.2.1. Laser Experiments

#### Laser Setup

All laser experiments were conducted using a *Coherent Opolette* 355 tuneable OPO, operated at wavelengths between 320 nm and 525 nm with a full width half maximum of 7 ns and a repetition rate of 20 Hz. The emitted pulse, which has a flat-top spatial profile, was expanded to 6 mm diameter using focussing lenses and directed upwards using a prism. The energy of the laser pulses was downregulated by an attenuator (polarizer). The beam was redirected into the vertical cylindrical hole of a custom-made sample holder, which contains the samples during the experiments (**Figure S 12**). These glass vials were crimped 0.7 mL vials by LLG Labware, Lab Logistic Group GmbH (Art. Nr. 4-008202). The energy of the incident laser pulses was measured by an Energy Max PC power meter (Coherent) directly above the sample holder. Prism and sample holder are positioned in a way that the complete diameter of the hole of the sample holder was covered by the incident laser beam.

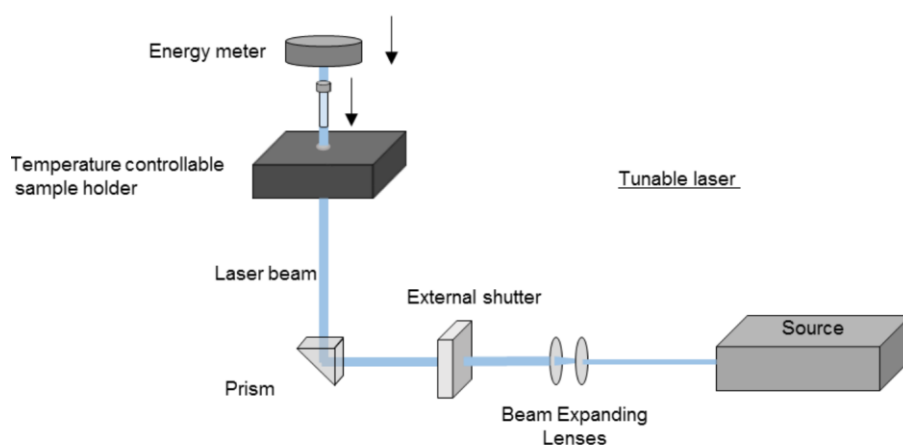


**Figure S 12** Experimental setup for the tuneable laser experiments. Energy output is adjusted using an attenuator and read out with an energy meter before the sample is inserted into the sample holder. Pulse energy is adjusted for each wavelength to ensure constant number of photons in every experiment.

## Control over Incident Photon Number<sup>1</sup>

The number of photons  $n_p$  ( $[n_p] = \text{mol}$ ) that a monochromatic laser pulse contains can be calculated by application of the Planck-Einstein relation from the energy of the pulse  $E_{\text{pulse}}$ , the incident wavelength  $\lambda$ , Planck's constant  $h$  and the speed of light  $c$ .

$$n_p = \frac{E_{\text{pulse}} \lambda}{h c N_A}$$

If the absorption of the glass vial and the extent of reflection and scattering at the vial at the respectively relevant wavelength is known, a target energy value can be calculated that must be reached during the above-described measurement to guarantee that the desired number of photons penetrates the sample solution during the subsequent irradiation. The wavelength dependent transmittance of the glass vials was determined experimentally using the above setup. Three glass vials were randomly selected as calibration vials. For varying wavelengths and in each case at a constant power output of the laser the energy was measured both with and without the calibration vials fitted into the sample holder. The top parts of these vials were cut off to minimize errors in the procedure, since only the bottom and sides of the glass vials would contribute significantly to the reduction of the photon flux that enters the solution.

The measured energy per pulse without a calibration vial in the sample holder is denoted as  $E_0$  and the measured energy per pulse with a calibration vial in the sample holder as  $E_n$ . The transmittance was calculated as the ratio of  $E_n$  to  $E_0$ . The average transmittance over the measurements of the three vials ( $T_\lambda$ ) was plotted together with the respective error (compare **Figure S 13**).

$$T_\lambda = \frac{E_n}{E_0}$$

The target energy per pulse  $E_0$  can be calculated directly from the wavelength  $\lambda$ , the number of pulses  $k$ , the transmittance of the glass vial at the respective wavelength  $T_\lambda$  and the desired total photon count  $n_p$ .

$$E_0 = \frac{n_p N_A h c}{k T_\lambda \lambda}$$

By controlling the target  $E_0$  at the respective wavelength, the number of photons that penetrate each sample solution of one set of experiments as described in the following subsections was guaranteed to be identical despite irradiation at different wavelengths.

### Transmittance of Glass Vials

Transmittance of the bottom of the glass vials used in this study were obtained analogously to a method reported previously.<sup>2</sup>

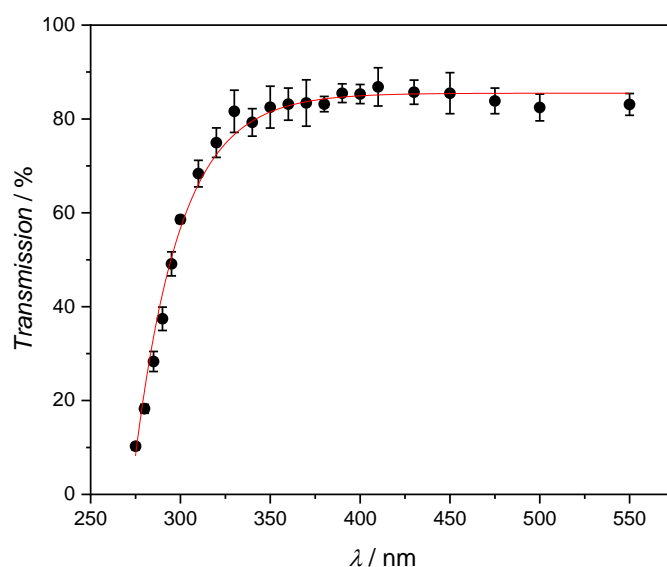


**Figure S 13** Calibration of the glass vial transmittance including a fit to obtain values that were not determined experimentally.

**Table S1** Transmittance of the glass vials used for the laser experiments.

$\lambda$ / nm	$T_{\lambda}$ / %	Mean Deviation / %
275	10.2	0.7
280	18.3	0.9
285	28.3	2.1
290	37.4	2.5
295	49.1	2.6
300	58.6	0.8
310	68.3	2.8
320	75.0	3.1
330	81.6	4.5
340	79.3	2.9
350	82.5	4.5
360	83.2	3.4
370	83.4	4.9
380	83.2	1.6
390	85.5	2.0
400	85.3	2.0
410	86.8	4.1
430	85.7	2.6
450	85.5	4.4
475	83.8	2.7
500	82.4	2.9
550	83.1	2.3

## Sample preparation for action plot measurements

APAT and diethylfumarate were employed in a 1:4 ratio, with the total concentration being 0.5 mg mL<sup>-1</sup> as per the LC-MS sample requirements. Sample solutions were freshly prepared every day and not kept overnight. Stock solutions (APAT: 0.46 mM; diethylfumarate: 1.84 mM in MeCN) were prepared and degassed with N<sub>2</sub> for 15 min, then 0.3 mL were withdrawn and added to capped photo vials that had previously been degassed with N<sub>2</sub> for 5 min. The samples were irradiated using the Coherent *Opolette* tuneable laser system and subsequently were filtered and directly used for LC-MS.

## Data of Laser Experiments

**Table S 2** Required laser pulse energy for each wavelength, resulting in a constant number of photons after irradiation for 15 min at a pulse rate of 20 Hz. <sup>a</sup>Because wavelengths between 300-400 nm are generated by sum frequency generation (SFG), laser output energies in this range are significantly reduced, giving pulse energies between 690 and 165  $\mu\text{J}$ . The lower pulse energy was compensated by adjusting the irradiation time for the indicated experiments accordingly (between 1 h to 3.5 h irradiation time).

Wavelength / nm	Photon Energy / J	Pulse Energy / mJ	Number of Photons / mol
320	6.21E-19	3.38 <sup>a</sup>	1.18E-4
340	5.84E-19	2.90 <sup>a</sup>	1.18E-4
360	5.52E-19	2.63 <sup>a</sup>	1.18E-4
380	5.23E-19	2.45 <sup>a</sup>	1.18E-4
400	4.97E-19	2.31 <sup>a</sup>	1.18E-4
410	4.84E-19	2.25	1.18E-4
420	4.73E-19	2.19	1.18E-4
430	4.62E-19	2.14	1.18E-4
440	4.51E-19	2.09	1.18E-4
450	4.41E-19	2.04	1.18E-4
455	4.37E-19	2.02	1.18E-4
460	4.32E-19	2.00	1.18E-4
465	4.27E-19	1.98	1.18E-4
470	4.23E-19	1.96	1.18E-4
475	4.18E-19	1.94	1.18E-4
480	4.14E-19	1.92	1.18E-4
490	4.05E-19	1.88	1.18E-4
500	3.97E-19	1.84	1.18E-4
510	3.89E-19	1.80	1.18E-4
515	3.86E-19	1.79	1.18E-4
525	3.78E-19	1.75	1.18E-4

## LC-MS Data Processing and Calculation of Conversion

LC-MS chromatograms (scan wavelength 392 nm) were plotted and processed using Origin 2018 64Bit®. Chromatograms were baseline corrected and the peaks of APAT and CA1 were integrated. A peak integral ratio  $r$  was calculated from the integrals by using the formula:  $r = \frac{I_{CA1}}{I_{APAT} + I_{CA1}}$

The difference in the molar absorption coefficients of APAT ( $\epsilon_{392\text{ nm}} = 9900\text{ L mol}^{-1}\text{ cm}^{-1}$ ) and CA1 ( $\epsilon_{392\text{ nm}} = 20000\text{ L mol}^{-1}\text{ cm}^{-1}$ ) was then taken into account to calculate the conversion.

**Table S 3** Results of the laser experiments. Reaction conversion was determined *via* LC-MS. Error bars were obtained through 3x repetition of every experiment. Due to very long irradiation time (refer to **Table S 2**) experiments between 320 nm and 400 nm were repeated 2x.

Wavelength / nm	Conversion / %	Standard Error / %
320	12.5	1.0
340	4.4	0.7
360	2.0	0.2
380	2.8	2.45
400	4.2	1.3
410	10.9	0.5
420	13.1	0.5
430	13.8	0.1
440	14.4	0.7
450	14.2	2.04
455	11.8	0.8
460	10.2	0.3
465	8.2	0.1
470	8.0	0.4
475	3.1	0.2
480	2.7	0.0
490	1.6	0.0
500	0.6	0.0

510	0.2	0.0
515	0.0	0.0
525	0.0	0.0

## 2.2.2. LED Experiments

LED experiments were conducted using 10 W LEDs centred around 452 nm, 500 nm or 515 nm, respectively. The prepared sample vials were placed on top of the LED in 10 mm distance using a custom-made sample holder. A magnetic stirrer was positioned underneath to enable stirring of the reaction mixture, and the LED was cooled using a compressed air flow.

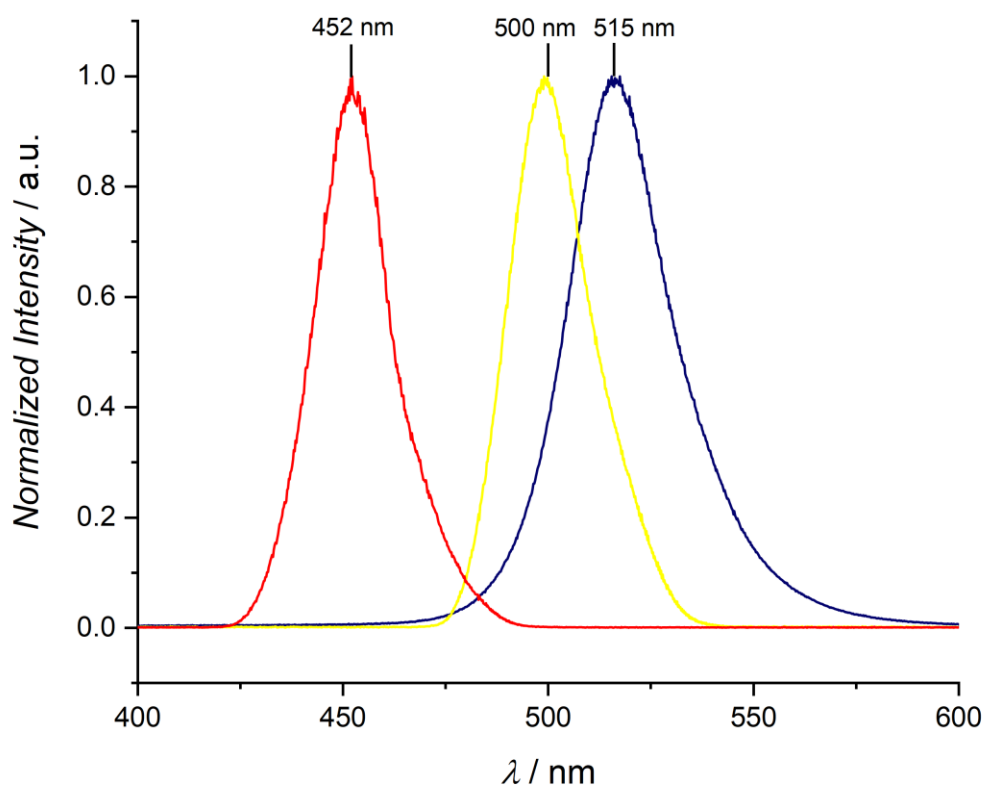


**Figure S 14** Emission spectra of 10 W LEDs used for photoreactions.

LED emission spectra were recorded using an Ocean Insight Flame-T-UV-Vis spectrometer, with an active range of 200-850 nm and an integration time of 10 ms. LED output energies were recorded using a Thorlabs S401C thermopile sensor, with an active area of 100 mm<sup>2</sup> and a wavelength range of 190 nm – 20 μm, connected to a Thorlabs PM400 energy meter console. The emitted power from each LED was measured for 60 seconds at a fixed distance from the sensor, after which the mean and standard deviation of the emission could be determined. LEDs were cooled during measurement to minimise any thermal effects on the emission power or sensor performance.

## 2.3. Synthesis

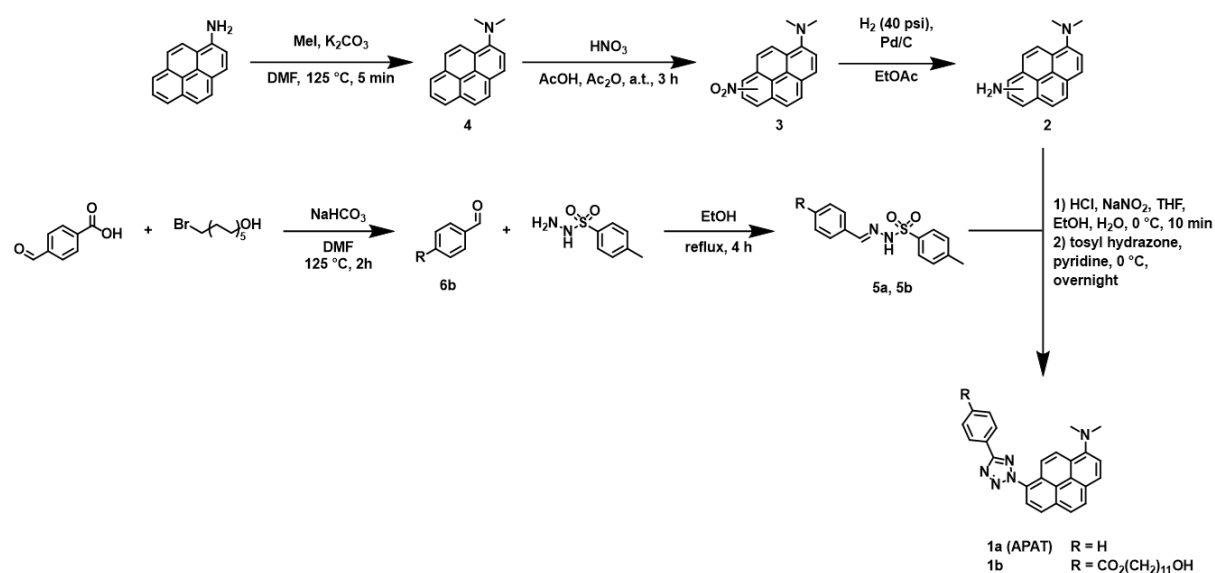
### 2.3.1. Materials

All chemicals were reagent or analytical grade and used as received, unless stated otherwise. 11-bromo-undecan-1-ol (98 %, Combi-Blocks), 1-aminopyrene (97 %, Sigma-Aldrich), 1-ethyl-3-(3-dimethylaminopropyl)carbodiimide hydrochloride (EDC, 98 %, Sigma-Aldrich), 4-(dimethylamino)pyridine (DMAP, >99 %, Sigma-Aldrich), 4-carboxybenzaldehyde (98 %, Thermo Fisher Scientific), 4-cyano-4-(phenylcarbonothioylthio)pentanoic acid (97 %, Sigma-Aldrich), acetic acid (glacial, AJAX FineChem), acetic anhydride (analytical grade, Chem Supply), acetonitrile (HPLC grade, Chem Supply), aluminium oxide activated basic (for chromatography, Thermo Fisher Scientific), azoazobisisobutyronitrile (AIBN, 12 w% in acetone, recrystallized from ethanol, Sigma-Aldrich), benzaldehyde (99 %, Sigma-Aldrich), chloroform (99.8 %, Thermo Fisher Scientific), chloroform-D (CDCl<sub>3</sub>, 99.8 % D, + silver foil, Nova Chem), cyclohexane (ACS grade, Merck), dichloromethane (analytical grade, Thermo Fisher Scientific), dimethyl sulfoxide-D (DMSO-d<sub>6</sub>, 99.9 % D, Nova Chem), dimethylformamide (99.8 %, Sigma-Aldrich), ethanol (analytical grade, AJAX FineChem), hydrochloric acid (32 w%, Thermo Fisher Scientific), iodomethane (laboratory grade, Chem Supply), magnesium sulfate anhydrous (>98 %, Merck), methanol (analytical grade, Thermo Fisher Scientific), methyl methacrylate (99 %, deinhibited by passing through a basic aluminium oxide column prior to use, Sigma-Aldrich), N,N-dimethylacetamide (99+ %, Thermo Fisher Scientific), nitric acid (65 w%, Thermo Fisher Scientific), palladium on carbon (10 w%, Sigma-Aldrich), potassium carbonate anhydrous (analytical grade, Chem Supply), p-toluenesulfonyl hydrazide (97 %, Sigma-Aldrich), pyridine (99 %, Sigma-Aldrich), sodium chloride (analytical grade, Thermo Fisher Scientific), sodium hydrogen carbonate (analytical grade, Thermo Fisher Scientific), sodium nitrite (97 %, Thermo Fisher Scientific), sodium sulfate anhydrous (analytical grade, Thermo Fisher Scientific), tetrahydrofuran (HPLC grade,

Thermo Fisher Scientific), toluene (analytical grade, Thermo Fisher Scientific), triphenylphosphine (99 %, Sigma-Aldrich).

Thin-layer chromatography (TLC) was performed on silica gel 60 F254 alumina sheets (Merck) and visualized by UV light. Column chromatography was run on an Interchim XS420 + SofTA Model 400 ELSD, or manually on silica gel 60 (0.04-0.06 mm, 230-400 mesh ASTM, Merck).

### 2.3.2. Dimethylaminopyrene aryl tetrazole (APAT)



**Scheme 5.1** Summarized reaction route for the synthesis of APAT (**1a**) and APAT equipped with a linker chain (**1b**).

### (E)-N'-benzylidene-4-methylbenzenesulfonohydrazide (tosyl hydrazone) **5a**

A solution of benzaldehyde (1.00 g, 9.42 mmol, 1.00 eq.) and toluene sulfone hydrazide (1.75 g, 9.42 mmol, 1.00 eq.) in EtOH (20 mL) was refluxed for 4 h and subsequently poured into H<sub>2</sub>O (100 mL). The precipitate was collected by filtration and dried in vacuum. The product was obtained as a white solid and used without further purification (2.55 g, 99%).

<sup>1</sup>H-NMR (600 MHz, DMSO-*d*<sub>6</sub>)  $\delta$  [ppm] = 11.43 (s, 1H), 7.90 (s, 1H), 7.80-7.71 (m, 2H), 7.59-7.49 (m, 2H), 7.46-7.32 (m, 5H), 2.35 (s, 3H).

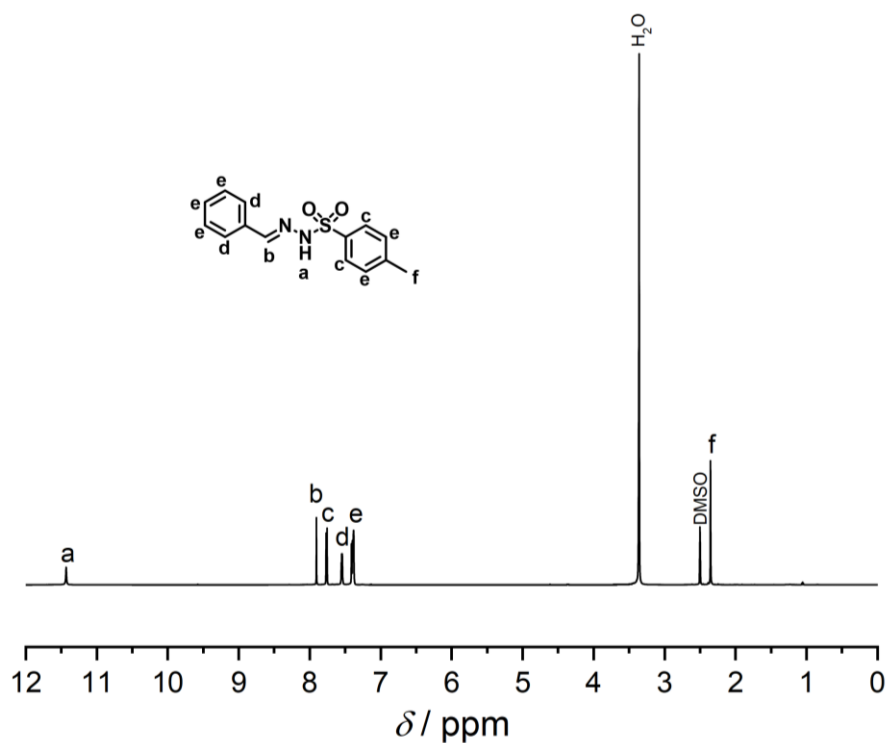


**Figure S 15** <sup>1</sup>H-NMR spectrum of **5a** in DMSO-*d*<sub>6</sub>.

### ***N,N*-dimethylpyren-1-amine **4****

Pyren-1-amine (4.96 g, 22.8 mmol, 1.00 eq.) and potassium carbonate (15.87 g, 114 mmol, 5.00 eq.) were combined in a round bottom flask and air was exchanged for argon. Dry DMF (30 mL) was added and, finally, iodomethane (7.11 mL, 16.2 g, 114 mmol, 5.00 eq.) was added dropwise over 10 min while stirring the brown solution. The flask was equipped with an argon filled balloon. Subsequently, the mixture was heated to 125 °C for 5 min and then allowed to cool down. Excessive iodomethane was quenched with 30 mL of MeOH, and the mixture was stirred for another 10 min. After ethyl acetate was added the mixture was extracted three times with water. The organic layer was dried over MgSO<sub>4</sub> and the solvent evaporated. The product was obtained as a brown oil and was used without further purification (5.27 g, 94 %).

<sup>1</sup>H-NMR (600 MHz, CDCl<sub>3</sub>) δ [ppm] = 8.48 (d, *J* = 9.2 Hz, 1H), 8.17-8.05 (m, 4H), 8.02-7.90 (m, 3H), 7.76 (d, *J* = 8.2 Hz, 1H), 3.07 (s, 6H).

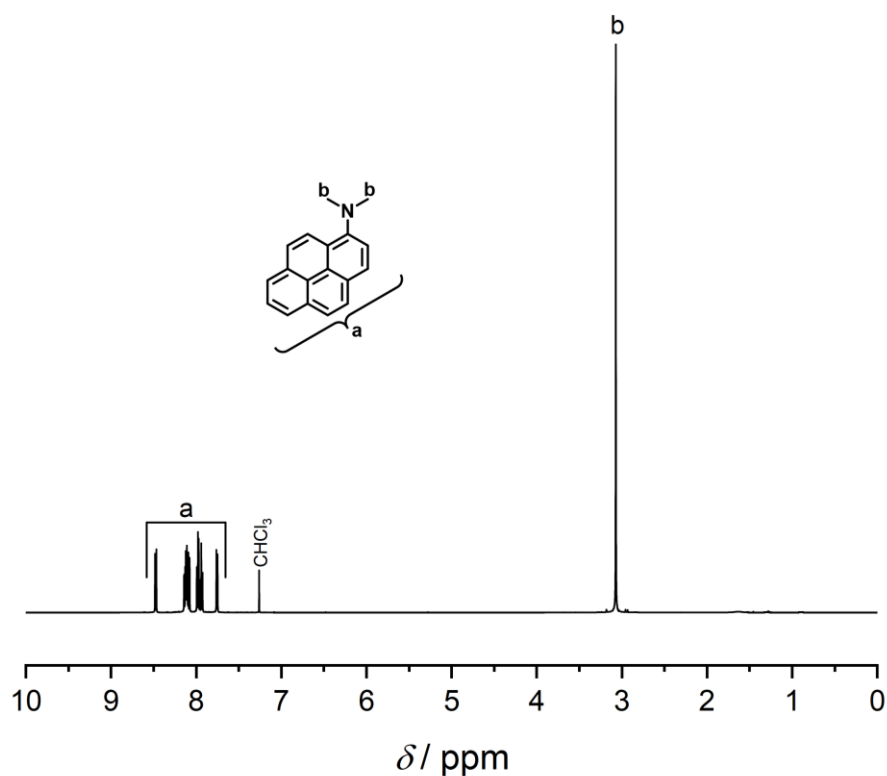


**Figure S 16** <sup>1</sup>H-NMR spectrum of **4** in CDCl<sub>3</sub>.

### ***N,N*-dimethyl nitropyren-1-amine 3**

**4** (3.53 g, 14.4 mmol, 1.00 eq.) was dissolved in acetic acid (200 mL) and acetic anhydride (55 mL). Under vigorous stirring, HNO<sub>3</sub> (1.68 mL, 65 w%, 2.37 g, 36.5 mmol, 1.70 eq.) in 10 mL AcOH was added dropwise over 1 h to the brown solution. TLC indicated presence of starting material ( $R_f = 0.7$  in CH/EA 4:1) and mono-nitrated product ( $R_f = 0.5$  in CH/EA 4:1). Another 0.3 eq. HNO<sub>3</sub> in 10 mL AcOH was added dropwise over an hour. This was repeated and each time the reaction was thoroughly monitored *via* TLC and <sup>1</sup>H-NMR spectroscopy to avoid formation of large amounts of double nitrated product. After a total amount of 2.5 eq. HNO<sub>3</sub> and 3.5 h reaction time, the mixture turned into a dark red and TLC indicated beginning formation of double nitrated product ( $R_f = 0.4$  in CH/EA 4:1). The reaction was quenched with 150 mL H<sub>2</sub>O. The mixture was extracted with chloroform four times and the organic layer washed with water twice, dried over MgSO<sub>4</sub> and filtered. The product was adsorbed onto Celite® filter agent and purified by column chromatography (silica, cyclohexane/ethyl acetate gradient (9:1 → 4:1 v/v)). Separation of regio-isomers was not achieved and the product contained *N,N*-dimethyl-8-nitropyren-1-amine, *N,N*-dimethyl-6-nitropyren-1-amine and *N,N*-dimethyl-3-nitropyren-1-amine in a ratio of 2:2:1, which was estimated from the relative peak integrals of the -NMe<sub>2</sub> signals in the <sup>1</sup>H-NMR spectrum. The product was obtained as a red powder (2.42 g, 58 %).

## **N,N-dimethylpyrene-1,8-diamine 2**

**3** (2.36 g, 8.13 mmol) was dissolved in 130 mL ethyl acetate and Pd/C (692 mg, 10 w%, 650  $\mu$ mol, 0.08 eq.) was added. After flushing with N<sub>2</sub> the vessel was filled with H<sub>2</sub> (40 psi) and shaken for 4 h. Over the course of the reaction, the mixture changed colour from dark red to blue with a yellow glint. The mixture was filtered over Celite® filter agent and the solvent was evaporated. The crude product was purified *via* Puriflash silica column (15  $\mu$ m, cyclohexane/ethyl acetate gradient (99:1  $\rightarrow$  4:1 v/v)). While the 1,3- and 1,6-substituted isomers were inseparable ( $R_f$  = 0.7 in CH/EA 1:1 v/v), a clean fraction of *N,N*-dimethylpyrene-1,8-diamine ( $R_f$  = 0.6 in CH/EA 1:1 v/v) was obtained. Position of the substituents was confirmed *via* NMR spectroscopy (<sup>1</sup>H-NMR and <sup>13</sup>C-NMR spectroscopy, correlation spectroscopy (COSY), heteronuclear multiple bond correlation (HMBC) and heteronuclear single-quantum correlation spectroscopy (HSQC)). The product was obtained as a brown oil (861 mg, 41 %,  $R_f$  = 0.6 in CH/EA 1:1 v/v).

<sup>1</sup>H-NMR (400 MHz, CDCl<sub>3</sub>)  $\delta$  [ppm] = 8.40 (d,  $J$  = 9.5 Hz, 1H), 8.02 (d,  $J$  = 8.2 Hz, 1H), 7.99-7.89 (m, 2H), 7.85-7.73 (m, 2H), 7.71 (d,  $J$  = 8.2 Hz, 1H) 7.31 (d,  $J$  = 8.1, 1H), 4.29 (b, 2H), 3.05 (s, 6H).

<sup>13</sup>C-NMR (150 MHz, CDCl<sub>3</sub>)  $\delta$  [ppm] = 147.61, 140.49, 128.16, 126.77, 126.50, 125.96, 125.53, 125.07, 124.39, 123.80, 119.37, 117.36, 116.56, 113.91, 45.65.

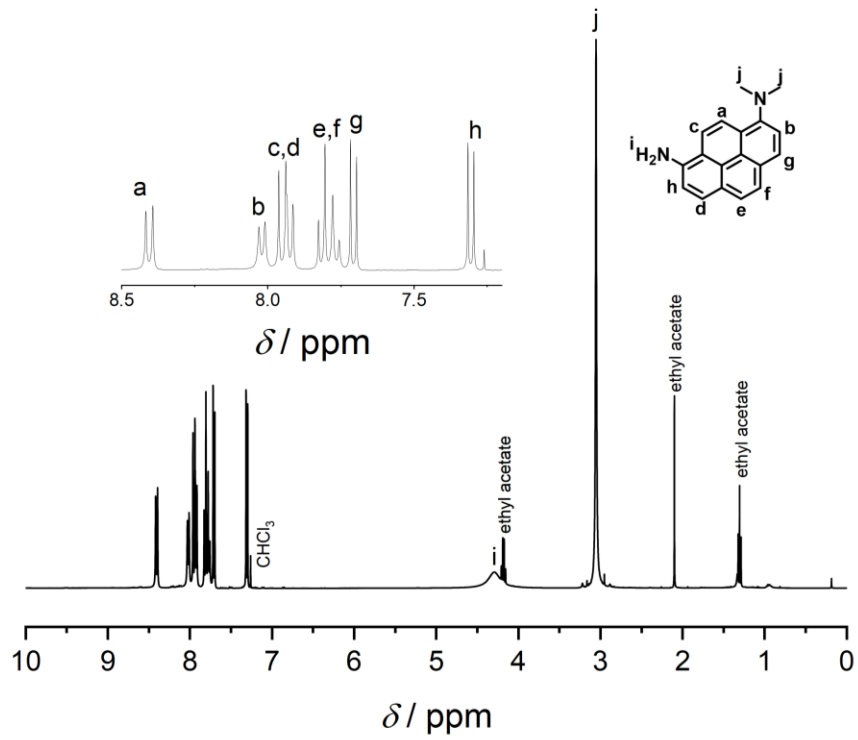


**Figure S 17**  $^1\text{H-NMR}$  spectrum of **2** in  $\text{CDCl}_3$ .

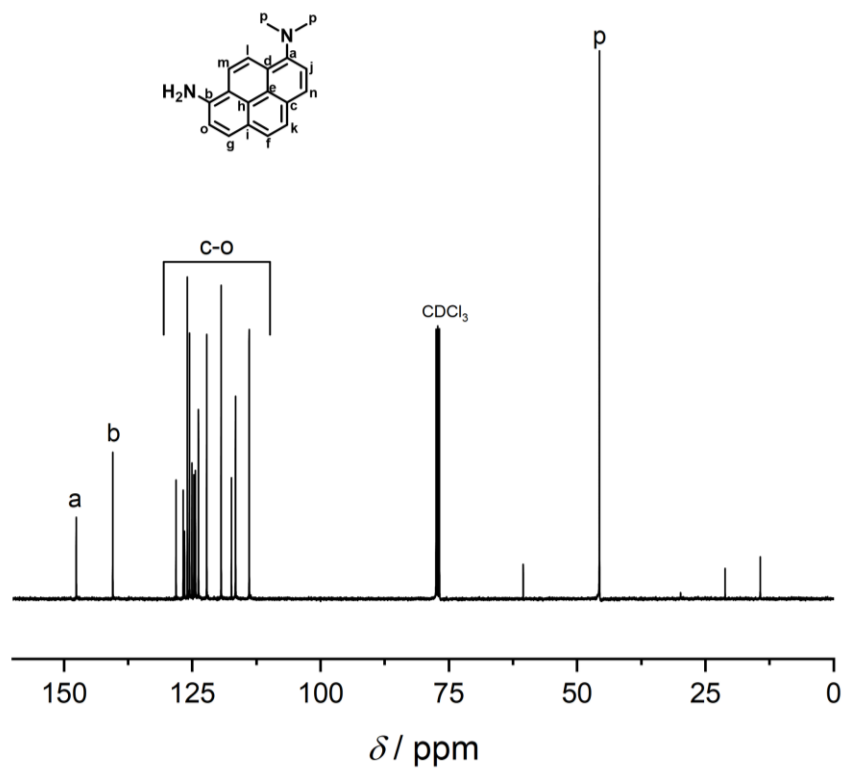


**Figure S 18**  $^{13}\text{C-NMR}$  spectrum of **2** in  $\text{CDCl}_3$ .

## **N,N-dimethyl-8-(5-phenyl-2H-tetrazol-2-yl)pyren-1-amine (APAT) 1a**

In a round bottom flask **2** (250 mg, 960  $\mu\text{mol}$ , 1.00 eq.) was dissolved in a mixture of EtOH, H<sub>2</sub>O (3 mL each) and HCl (294  $\mu\text{L}$ , 37 w%, 3.46 mmol, 3.60 eq.) and cooled to -10 °C in an ice/salt mixture. In parallel, a solution of **5a** (610 mg, 1.25 mmol, 1.30 eq.) in pyridine (6 mL) was prepared and likewise cooled to -10 °C. To the aqueous mixture was added NaNO<sub>2</sub> (66.3 mg, 960  $\mu\text{mol}$ , 1.00 eq.) in a minimum amount of ice-cold water dropwise while vigorously stirring. The yellow mixture immediately turned dark blue and was continuously cooled and stirred for 10 min. Subsequently, the blue diazonium salt solution was quickly transferred to the cooled pyridine solution and the flask rinsed with 6 mL of cooled pyridine (-10 °C). The reaction flask was covered and allowed to warm up to ambient temperature overnight. Subsequently, the now red mixture was poured into 100 mL of 1M HCl and stirred for one hour. Ethyl acetate was added, and the product extracted and washed with H<sub>2</sub>O until the aqueous layer was neutral. The organic layer was dried over Mg<sub>2</sub>SO<sub>4</sub>, filtered, and evaporated. The crude product was purified *via* Puriflash silica column (30  $\mu\text{m}$ , cyclohexane/ethyl acetate gradient (99:1  $\rightarrow$  95:1 v/v)). Finally, the product was recrystallized from MeCN to obtain a yellow powder (110 mg, 29 %, R<sub>f</sub> = 0.7 in CH/Ea 4:1 v/v).

<sup>1</sup>H-NMR (600 MHz, CDCl<sub>3</sub>)  $\delta$  [ppm] = 8.58 (d,  $J$  = 9.6 Hz, 1H), 8.40-8.35 (m, 2H), 8.35-8.29 (m, 2H), 8.25-8.19 (d,  $J$  = 8.2 Hz, 2H), 8.12 (d,  $J$  = 8.9 Hz, 1 H), 8.00 (d,  $J$  = 8.8 Hz, 1H), 7.81 (d,  $J$  = 8.3 Hz, 1H), 7.62-7.51 (m, 3H), 3.09 (s, 6H).

<sup>13</sup>C-NMR (150 MHz, CDCl<sub>3</sub>)  $\delta$  [ppm] = 165.45, 150.44, 133.54, 130.72, 129.39, 127.31, 126.45, 125.03, 124.12, 122.96, 120.27, 117.36, 45.81.

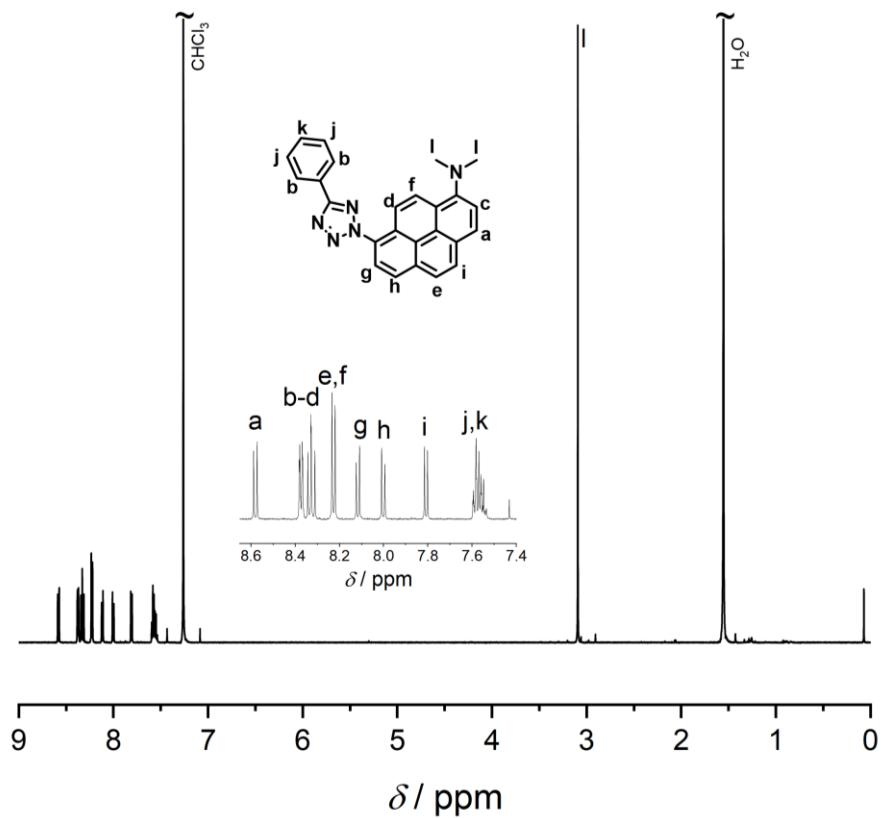


**Figure S 19**  $^1\text{H-NMR}$  spectrum of APAT (**1a**) in  $\text{CDCl}_3$ .

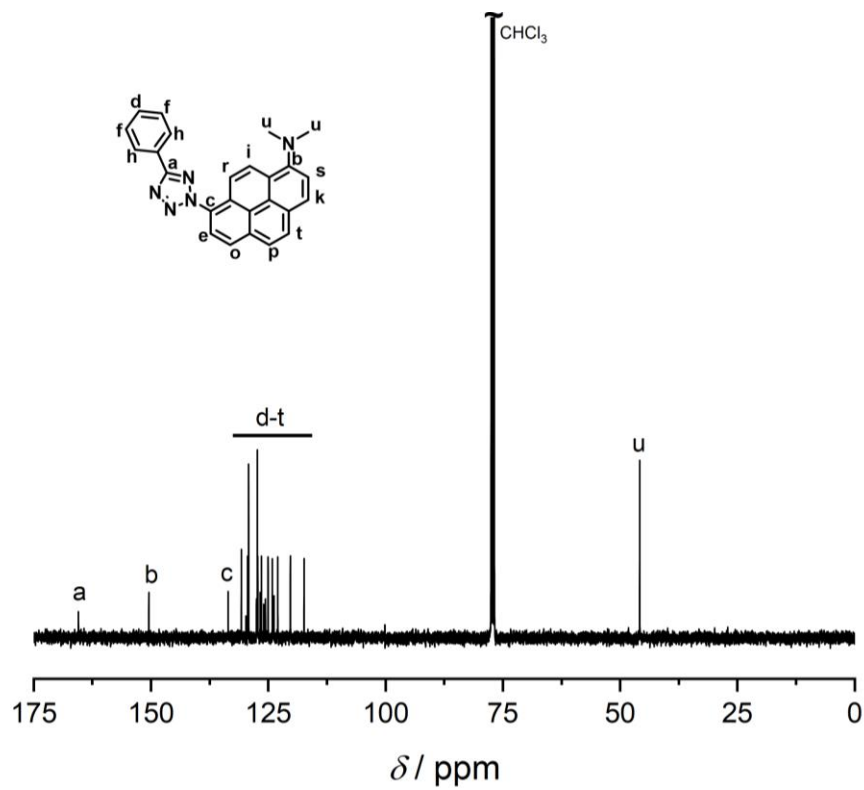


**Figure S 20**  $^{13}\text{C-NMR}$  spectrum of APAT (**1a**) in  $\text{CDCl}_3$ .

## 11-hydroxyundecyl 4-formylbenzoate **6b**

In a round bottom flask 4-formyl benzoic acid (1.00 g, 6.66 mmol, 1.00 eq.), 11-bromo undecane-1-ol (2.18 g, 8.66 mmol, 1.30 eq.) and  $\text{NaHCO}_3$  (1.12 g, 13.3 mmol, 2.00 eq.) were dissolved in 10 mL DMF and heated to 125 °C for 2 h while stirring. After cooling down, the mixture was filtered, ethyl acetate (100 mL) was added and the organic layer was washed with brine (3x 50 mL) and  $\text{H}_2\text{O}$  (50 mL). The organic layer was dried over  $\text{Na}_2\text{SO}_4$  and the solvent evaporated. The product was obtained as a pale-yellow oil and used without further purification (2.13 g, 99 %)

$^1\text{H-NMR}$  (600 MHz,  $\text{CDCl}_3$ )  $\delta$  [ppm] = 10.10 (s, 1H), 8.19 (d,  $J = 8.1$  Hz, 2H), 7.95 (d,  $J = 8.1$  Hz, 2H), 4.35 (t,  $J = 6.7$  Hz, 2H), 3.63 (t,  $J = 6.6$  Hz, 2H), 1.78 (p,  $J = 6.9$  Hz, 2H), 1.58-1.52 (m, 2H), 1.47-1.41 (m, 2H), 1.33-1.25 (m, 12H).

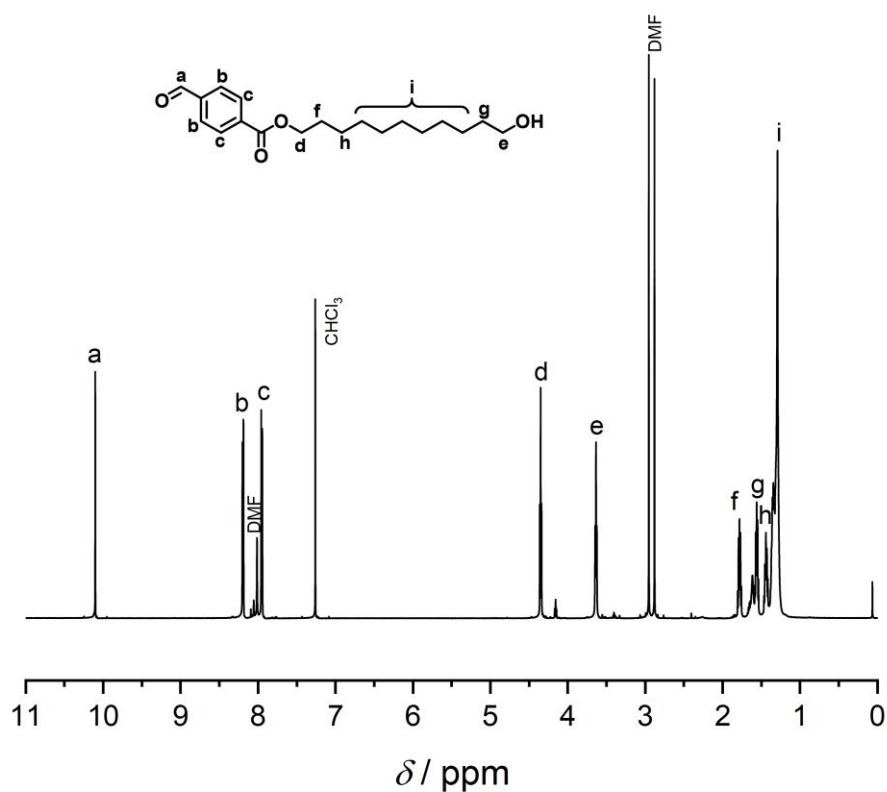


**Figure S 21**  $^1\text{H-NMR}$  spectrum of **6b** in  $\text{CDCl}_3$ .

## 11-hydroxyundecyl (*E*)-4-((2-tosylhydrazineylidene)methyl)benzoate **5b**

**6b** (2.13 g, 6.65 mmol, 1.00 eq.) was dissolved in EtOH (20 mL) and toluene sulfone hydrazide (1.36 g, 7.31 mmol, 1.10 eq.) was added. The mixture was stirred at ambient temperature overnight. The solvent was evaporated, and the product was purified *via* silica column chromatography (2 % MeOH in DCM). After drying, the product was obtained as a white solid (2.01 g, 62 %,  $R_f = 0.1$  in MeOH/DCM 2:98 v/v).

$^1\text{H-NMR}$  (600 MHz,  $\text{DMSO-}d_6$ )  $\delta$  [ppm] = 11.71 (b, 1H), 7.94 (d,  $J = 8.3$  Hz, 2H), 7.76 (d,  $J = 8.1$  Hz, 2H), 7.68 (d,  $J = 8.3$  Hz, 2H), 7.41 (d,  $J = 8.1$  Hz, 2H), 4.31 (s, 1H), 4.25 (t,  $J = 6.5$  Hz, 2H), 2.36 (s, 3H), 1.69 (p,  $J = 6.8$  Hz, 2H), 1.44-1.34 (m, 2H), 1.34-1.16 (m, 14 H).

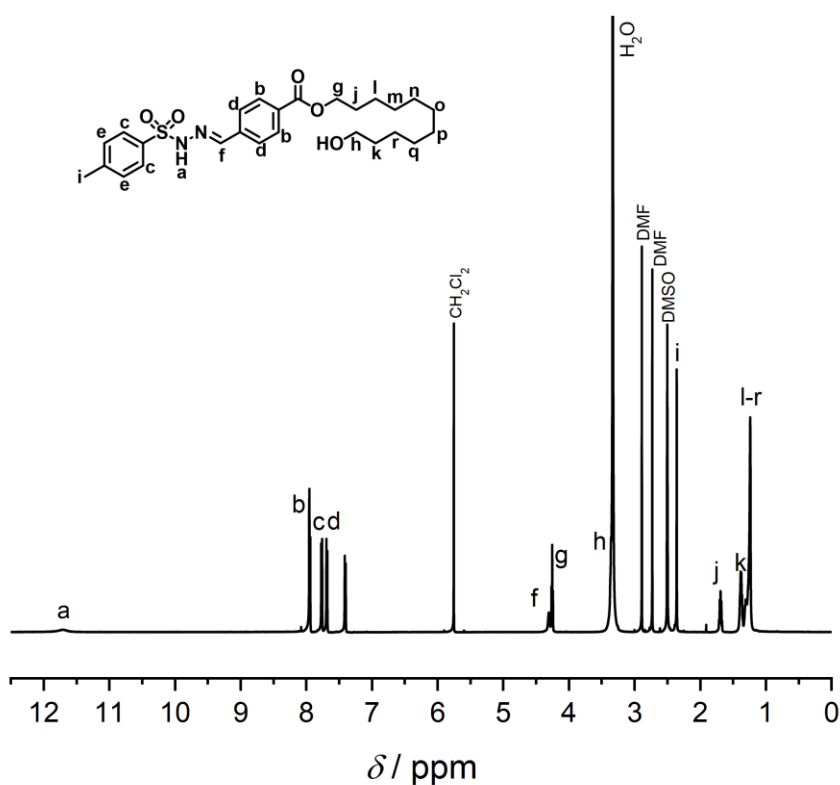


**Figure S 22**  $^1\text{H-NMR}$  spectrum of **5b** in  $\text{DMSO-}d_6$ .

**11-hydroxyundecyl 4-(2-(8-(dimethylamino)pyren-1-yl)-2H-tetrazol-5-yl)benzoate (APAT-linker) 1b**

In a round bottom flask **2** (250 mg, 960  $\mu\text{mol}$ , 1.00 eq.) was dissolved in a mixture of EtOH, H<sub>2</sub>O (3 mL each) and HCl (294  $\mu\text{L}$ , 37 w%, 3.46 mmol, 3.60 eq.) and cooled to -10 °C in an ice/salt mixture. In parallel, a solution of **5b** (610 mg, 1.25 mmol, 1.30 eq.) in pyridine (6 mL) was prepared and likewise cooled to -10 °C. To the aqueous mixture was added NaNO<sub>2</sub> (66.3 mg, 960  $\mu\text{mol}$ , 1.00 eq.) in a minimum amount of ice-cold water dropwise while vigorously stirring. The yellow mixture immediately turned dark blue and was continuously cooled and stirred for 10 min. Subsequently, the blue diazonium salt solution was quickly transferred to the cooled pyridine solution and the flask rinsed with 6 mL of cooled pyridine (-10 °C). The reaction flask was covered and allowed to warm up to ambient temperature overnight. Subsequently, the now red mixture was poured into 100 mL of 1M HCl and stirred for one hour. Ethyl acetate was added, and the product extracted and washed with H<sub>2</sub>O until the aqueous layer was neutral. The organic layer was dried over Mg<sub>2</sub>SO<sub>4</sub>, filtered, and evaporated. The crude product was purified *via* silica column chromatography (cyclohexane/ethyl acetate gradient (4:1  $\rightarrow$  2:1 v/v)). Finally, the product was recrystallized from MeCN to obtain a yellow powder (140 mg, 24 %, R<sub>f</sub> = 0.53 in CH/Ea 3:2 v/v).

<sup>1</sup>H-NMR (600 MHz, CDCl<sub>3</sub>)  $\delta$  [ppm] = 8.61 (d,  $J$  = 9.6 Hz, 1H), 8.49-8.40 (m, 2H), 8.36-8.29 (m, 2H), 8.27-8.19 (m, 4H), 8.12 (d,  $J$  = 8.8 Hz, 1 H), 8.00 (d,  $J$  = 8.9 Hz, 1H), 7.82 (d,  $J$  = 8.3 Hz, 1H), 4.38 (t,  $J$  = 6.7 Hz, 2H), 3.64 (t,  $J$  = 6.6 Hz, 2H), 3.10 (s, 6H), 1.82 (dt,  $J$  = 6.8 Hz, 2H), 1.57 (dt,  $J$  = 8.2, 6.6 Hz, 2H), 1.51-1.45 (m, 2H), 1.43 – 1.25 (m, 12 H).

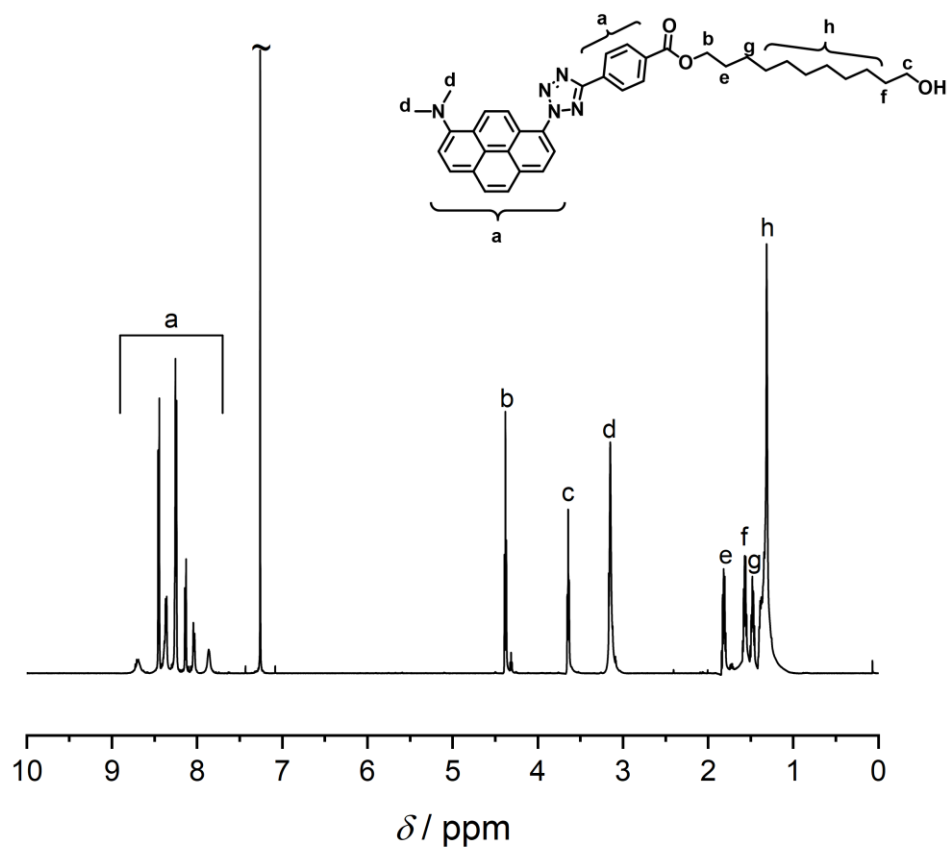
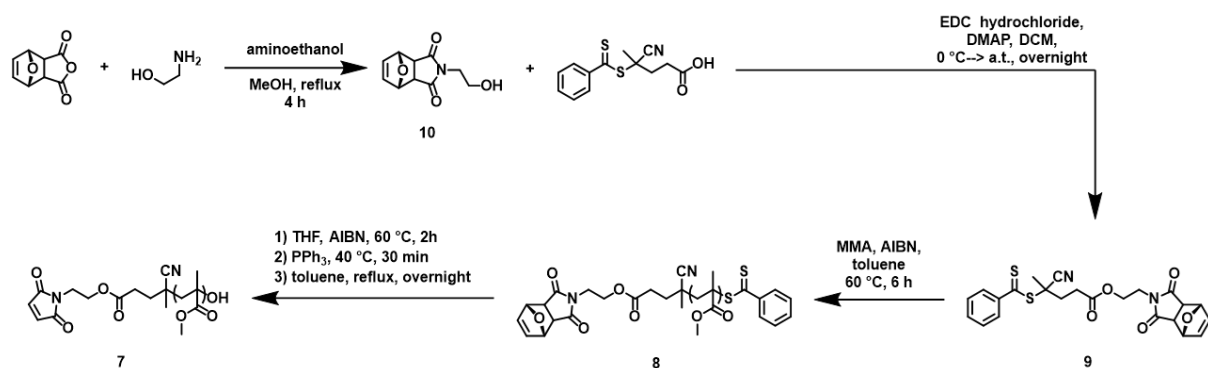


**Figure S 23**  $^1\text{H-NMR}$  spectrum of **1b** in  $\text{CDCl}_3$ .

### 2.3.3. Maleimide end-capped poly(methyl)methacrylate



**Scheme 5 2** Summarized reaction route for the synthesis of a maleimide-end-capped poly(methyl)methacrylate.

## Furan-protected *N*-(2-hydroxyethyl) maleimide **10**

Furan-protected maleic anhydride (1.50 g, 9.03 mmol, 1.00 eq.) was suspended in 45 mL MeOH and cooled to 0 °C. A solution of 2-aminoethanol in 15 mL MeOH was added dropwise over 15 min, and the mixture was allowed to warm up to room temperature and finally refluxed for 4 h. The solvent was evaporated and the product was recrystallized from MeOH to yield a white solid (673 mg, 35 %).

$^1\text{H-NMR}$  (600 MHz,  $\text{CDCl}_3$ )  $\delta$  [ppm] = 6.52 (d,  $J = 0.9$  Hz, 2H), 5.28 (dd,  $J = 1.0$  Hz, 2H), 3.80-3.74 (m, 2H), 3.74-3.68 (m, 2H), 2.89 (d,  $J = 0.8$  Hz, 2H).

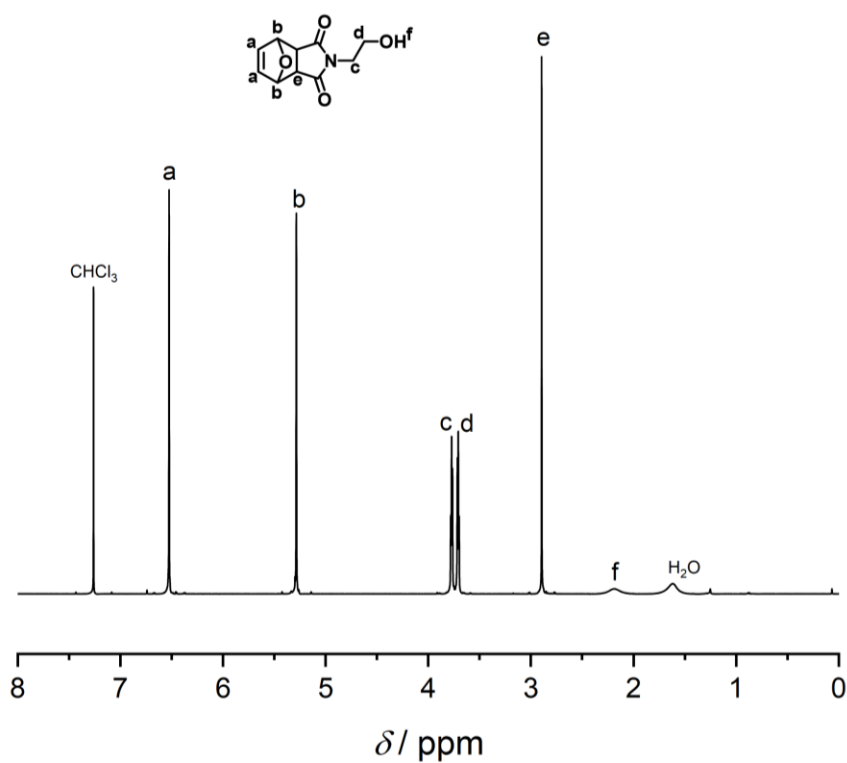


**Figure S 24**  $^1\text{H-NMR}$  spectrum of **10** in  $\text{CDCl}_3$ .

**2-((4R,7S)-1,3-dioxo-1,3,3a,4,7,7a-hexahydro-2H-4,7-epoxyisoindol-2-yl)ethyl-4-cyano-4-((phenylcarbonothioyl)thio)pentanoate (chain-transfer agent, CTA) 9**

4-cyano-4-((phenylcarbonothioyl)thio)pentanoic acid (572 mg, 2.05 mmol, 1.20 eq.) was added to a Schlenk tube and air was exchanged for argon in three cycles. Dry DCM (20 mL) and **10** (357 mg, 1.71 mmol, 1.00 eq.) were added and the solution was cooled to 0 °C. Finally, EDC·HCl (527 mg, 2.56 mmol, 1.50 eq.) and DMAP (31.3 mg, 256 μmol, 0.15 eq.) were added and the mixture was stirred at 0 °C for two hours, then overnight at ambient temperature. Subsequently, DCM was added, and the solution was extracted with water and brine. The organic layer was dried over MgSO<sub>4</sub> and the solvent evaporated under vacuum at 25 °C, due to the heat sensitivity of the product. The product was purified *via* Puriflash silica column (cyclohexane / ethyl acetate gradient, 7:3 → 1:1 v/v). The product was obtained as a red oil (570 mg, 71 %).

<sup>1</sup>H-NMR (600 MHz, CDCl<sub>3</sub>) δ [ppm] = 8.00-7.84 (m, 2H), 7.57 (t, *J* = 7.4 Hz, 1H), 7.46-7.34 (m, 2H), 6.50 (d, *J* = 5.6 Hz, 2H), 5.26 (dd, *J* = 7.1 Hz, 1.5 Hz, 2H), 4.36-4.19 (m, 2H), 3.85-3.64 (m, 2H), 2.91-2.83 (m, 2H), 2.72-2.33 (m, 4H), 1.93 (s, 3H).

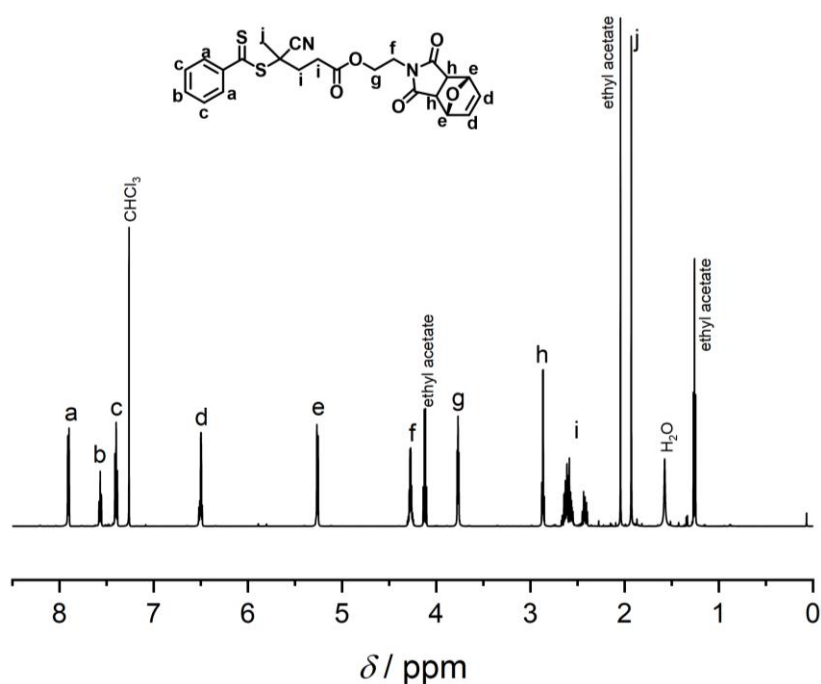


**Figure S 25** <sup>1</sup>H-NMR spectrum of **9** in CDCl<sub>3</sub>.

## Furan-protected maleimide end-capped poly(methyl)methacrylate **8**

**9** (188 mg, 398  $\mu\text{mol}$ , 1.00 eq.) and azobisisobutyronitrile (AIBN, 13.1 mg, 79.7  $\mu\text{mol}$ , 0.20 eq.) were added to a crimp vial equipped with a stirring bar. Using syringe needles, argon was flushed through for 15 min. Dry toluene (4.24 mL), that had previously been degassed with  $\text{N}_2$  for 1 h, and methylmethacrylate (3.99 g, 39.9 mmol, 100 eq.) (deinhibited by passing through a basic aluminium oxide column, then degassed with  $\text{N}_2$  for 5 min). A large excess of monomer was used to ensure high end-group fidelity. The mixture was again flushed with  $\text{N}_2$  in an ice bath, and subsequently emerged into a heating block at 60  $^\circ\text{C}$  while stirring. After 6 h the reaction was stopped by exposing the reaction mixture to air and freezing in liquid  $\text{N}_2$ . Solvent and remaining monomer were evaporated *in vacuo*. The resulting oil was dissolved in a small amount of THF and precipitated twice into cold MeOH (600 mL), then dried *in vacuo*. The product was obtained as a light pink solid (1.18 g).  $^1\text{H-NMR}$  spectroscopy was used to determine degree of polymerization and molecular weight ( $\text{DP} = 46$ ,  $M_n = 5.1$  kDa).

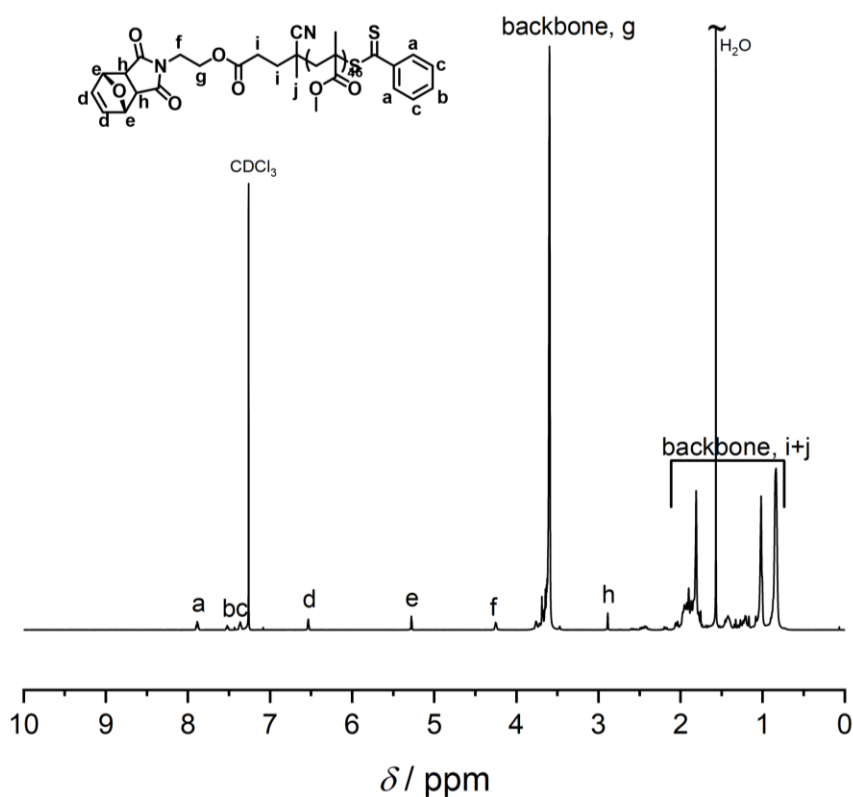


**Figure S 26**  $^1\text{H-NMR}$  spectrum of **8** in  $\text{CDCl}_3$ .

## ( $\omega$ -hydroxy) Maleimide end-capped poly(methyl)methacrylate **7**

AIBN (55 mg, 355  $\mu$ mol, 1.50 eq.) was dissolved in 30 mL THF and heated to 60  $^{\circ}$ C for 1 h. **8** (1.18 g, 224  $\mu$ mol, 1.00 eq.) was added and stirred for 1 h. 44 mg more AIBN was added and the solution was continuously stirred for one more hour, at which point the temperature was lowered to 1 h and PPh<sub>3</sub> (176 mg, 671  $\mu$ mol, 3.00 eq.) was added. After stirring for 30 min, the solvent was evaporated, the residue was dissolved in a minimum amount of THF and precipitated into cold MeOH. The white solid was dissolved in 60 mL toluene and heated to 110  $^{\circ}$ C overnight. The solvent was evaporated and the residue was precipitated into cold MeOH (500 mL). The product was obtained as a white solid (596 mg,  $M_n$ (NMR) = 5.2 kDa,  $M_n$ (SEC) = 4.7 kDa,  $D$  = 1.16). The <sup>1</sup>H-NMR spectrum revealed loss of the RAFT end-group as well as the furan protection group.

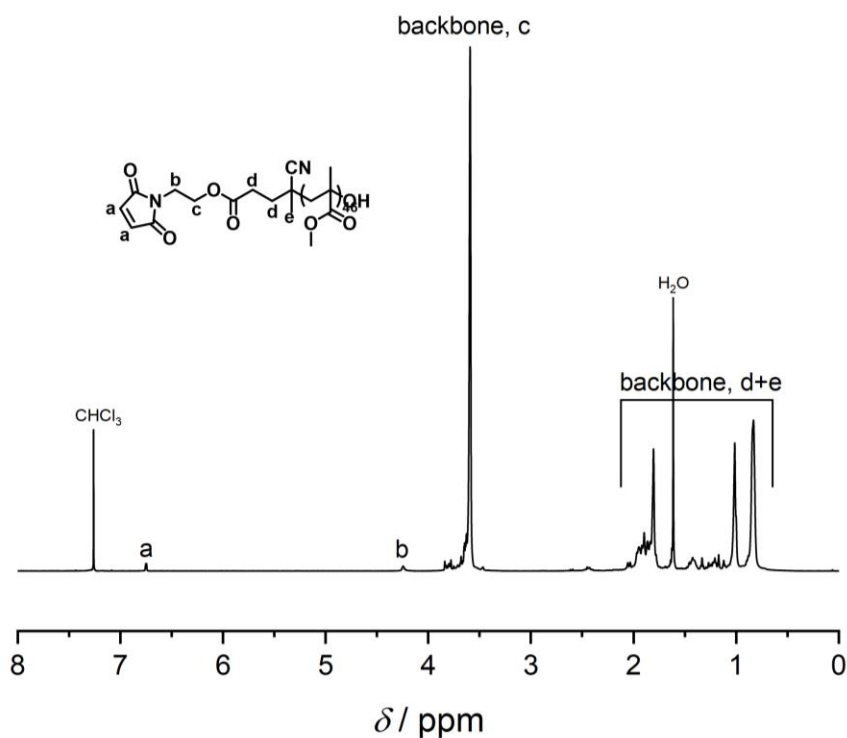


**Figure S 27** <sup>1</sup>H-NMR spectrum of **7** in CDCl<sub>3</sub>.

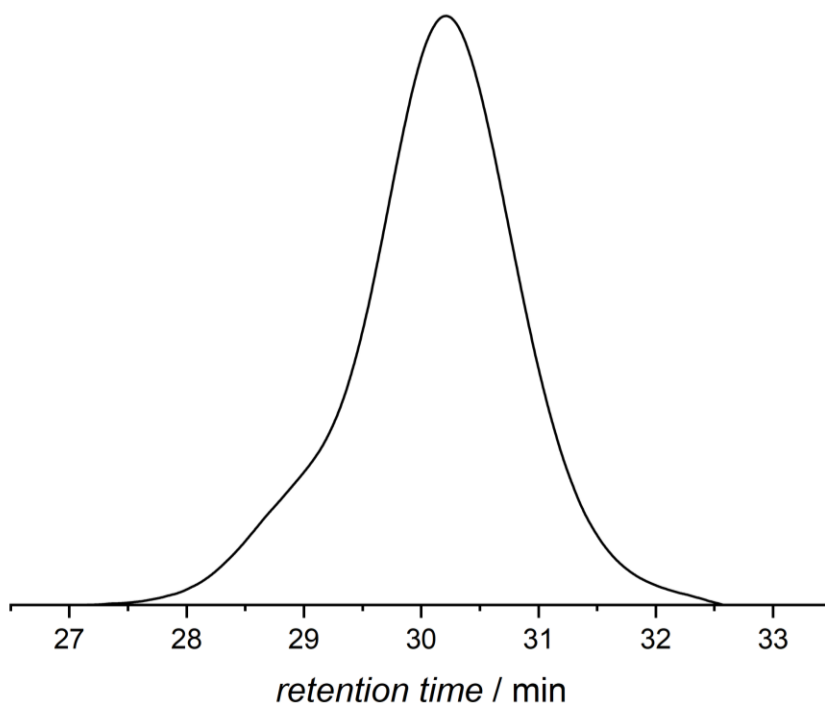


**Figure S 28** DMAc SEC trace of maleimide end-capped PMMA obtained through RAFT polymerization, employing **8** as a chain-transfer agent. ( $M_n = 5.2$  kDa ( $^1\text{H-NMR}$ ),  $M_n = 4.7$  kDa (SEC),  $\mathcal{D} = 1.16$ ).

### 3. Supporting References

- [1] D. E. Marschner, Frisch, H., Offenloch, J. T., Tuten, B. T., Becer, C. R., Walther, A., Goldmann, A. S., Tzvetkova, P., Barner-Kowollik, C., *Macromolecules* **2018**, *51*, 3802-3807.
- [2] J. P. Menzel, Noble, B. B., Lauer, A., Coote, M. L., Blinco, J. P., Barner-Kowollik, C., *Journal of the American Chemical Society* **2017**, *139*, 15812-15820.